Ocean and Sea Ice SAF

Technical Report
SAF/OSI/KNMI/TEC/RP/092

Scatterometer calibration tool development

Jeroen Verspeek

DRAFT - 20 August 2006

Summary

An ocean calibration tool is developed for the calibration of the forthcoming ASCAT scatterometer on board of the METOP satellite. Besides handling ASCAT data the tool is also capable of handling scatterometer data from the ERS satellite, the predecessor of METOP. In this report the ocean calibration method is described and the results from ERS runs and error simulation are presented.

The calibration method is based on Fourier analysis of the data and has also been used by [STOFFELEN 1998] and [HERSCHBACH 2003]. The aim of ocean calibration is, by comparing the average measured backscatter from the antennae to the simulated backscatter from collocated NWP winds, to assess the absolute values of the measurements and the GMF and to show that there is no interbeam bias. The calibration software is used with existing ERS data and with simulated ASCAT data. The method will be applied for ASCAT as soon as real ASCAT data becomes available.

First the calibration is described from a theoretical point of view, deriving the calculation of Fourier coefficients out of a measurement set. Then the calibration software itself and the way this method is implemented is described in more detail. Then examples of a typical ocean calibration are shown using a standard input data set from ERS, July 1999. The backscatter differences are in the order of a few tenth of a dB.

In the next section the input parameters, especially the wind distribution and the backscatter distribution are examined in more detail. Calibration results for different weighting method, different input data period, and different GMF are presented. Good agreement between the different weighting methods is found.

A simulation tool which produces BUFR data files with errors added to wind speed or to the backscatter is described. These errors are random but have a well defined probability distribution. Subsequently these BUFR files are used in a simulation run of the ocean calibration in order to assess the influence of the errors in the calibration process. A simulation run with realistic values for the instrument noise and the geophysical noise, and for the NWP wind component errors is performed. The results show that the impact of the wind component errors on the calibration is the largest, as compared to the impact of the instrument noise and the geophysical noise. The ocean calibration differences between real and simulated data need to be further investigated.

The output from the ocean calibration over a certain period can be used to correct biases in the ocean calibration over another period. The impact of such a correction is examined, and it is shown that for ERS the calibration results are stable over a longer period of time.

Contents

1 Introduction

The Advanced Scatterometer (ASCAT) will be part of the payload of the METOP satellite series satellites of which the first one will be launched in October 2006 (see Figure 1).

A scatterometer is an active radar instrument that measures the backscatter (σ^0) from the ocean surface from several radar pulses. Over sea, this backscatter is a function of the roughness and waves that are induced by wind. The empirical geophysical model function (GMF) relates the wind speed and wind direction with the backscatter. An example of a GMF is CMOD5 which is currently used to process ERS scatterometer data (see [HERSBACH 2003]). AMI and ASCAT are C-band scatterometers using V-pol fan beams with fixed geometry (see Figure 2). Each point in the swath is scanned three times successively by the fore-, mid- and aft antenna when the satellite passes over. Each measurement in space/time is represented by a triplet of σ^0-values from the antennae. ASCAT has a two sided swath and AMI a one sided swath. For ASCAT the swath is located somewhat further away from the nadir ground track compared to AMI, giving rise to higher incidence angles. Incidence angles range from [27.4°..63.9°] for ASCAT against [18°..56.5°] for ERS. Effectively the lower 5 ERS nodes are eliminated and 7 nodes are added at the high end of the incidence angle range.

A GMF inversion procedure is used to translate the measured backscatter values over the ocean into 10m wind speed and wind direction. Because of non-linearities of the GMF and measurement errors, the inversion provides a set of ambiguous wind solutions rather then a unique solution. Subsequently, an ambiguity removal procedure e.g. median filter (see [JPL 2001]) or 2D-VAR is used to retrieve the observed wind field and flags are set to indicate the quality of the retrievals.

Calibration of the absolute value of the level 1B backscatter is done using fixed targets on the ground. The ocean calibration on the other hand is independent from the former and uses the level 1B backscatter data above the ocean as input. A relatively short period of time (e.g. one day) of data is required to perform an independent ocean calibration. The software is prepared for ASCAT nominal (50 km footprint) and high resolution mode (25 km footprint) data.

In an ocean calibration essentially a set of measured σ^0-values is compared with an independent set, usually a collocated NWP wind field. All calibrations in this report have been done with ECMWF ERA40 collated wind fields. A typical calibration uses from one day to one month of scatterometer data. In a standard calibration run the first set contains σ^0-values measured by the scatterometer σ^0_m, the second set contains triplets derived from collocated NWP winds, using a geophysical model function (GMF) to transform the NWP winds into backscatter triplets σ^0_s. The σ^0-values are averaged resolved per antenna and per WVC or incidence angle θ. Then the differences in σ^0-values are compared.

In order to calibrate the ASCAT instrument, software has been developed. The software is tested with data from its predecessor the Active Microwave Instrument (AMI) scatterometer on board of the currently operational European Remote-Sensing satellite (ERS-2). In this report, a new calibration tool is presented that works for ERS and ASCAT. Additional tools have been developed to analyse oceanc calibration and simulate performance for ASCAT. In section 2 the ocean calibration method is described, in section 3 the tools are presented. Section 4 gives the analysis on ERS data and on data with simulated errors. Section 5 gives the conclusion and outlook.

This report is written within the framework of the OSI SAF IOP work package 23130 and 23250.

Figure 1 – METOP in orbit with the six ASCAT antennae clearly visible (picture ESA)

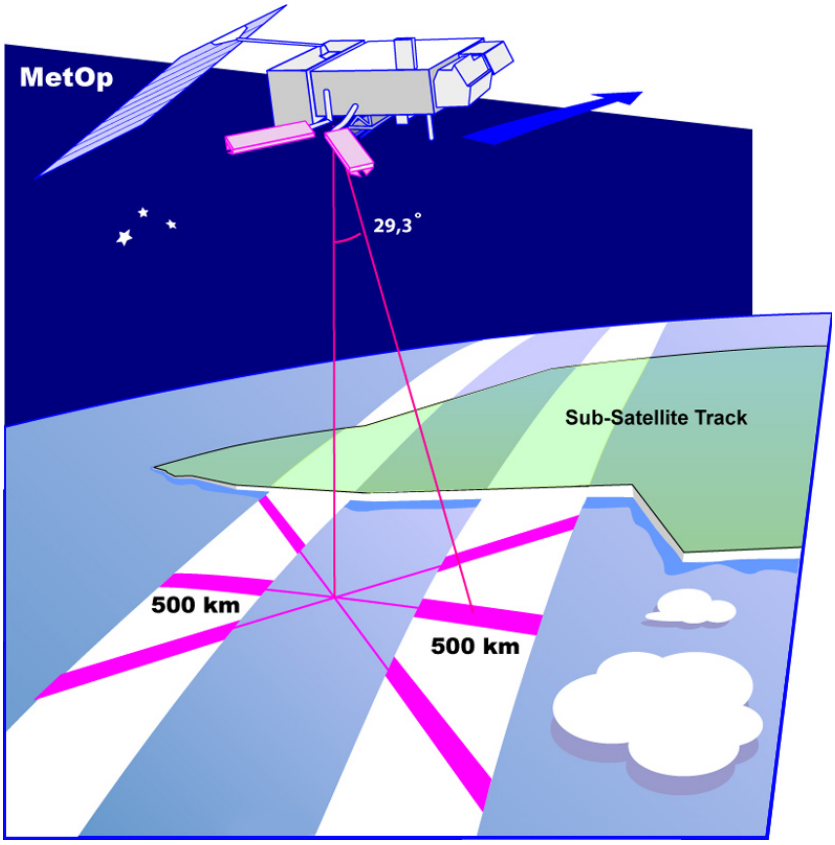

Figure 2 – ASCAT left and right swath

2 Method

In this section a description of the theoretical method to calculate the ocean calibration coefficients is given. The ocean calibration that is used in this document is based on the method described by [STOFFELEN 1998] and [HERSBACH 2003]. The method is based on a Fourier analysis of a large data set to estimate the Fourier coefficients of the GMF. Consider the CMOD5 GMF σ^0 (θ, V, Φ):

$$\sigma^0_{linear}(\theta, V, \phi) = B_0(\theta, V)[1 + B_1(\theta, V)\cos(\phi) + B_2(\theta, V)\cos(2\phi)]^{1.6}$$

Equation 1

When the GMF is transformed to z-space, i.e. $z=(\sigma^0_{linear})^{0.625}$, the Fourier expansion is limited to the second order with respect to the azimuth angle Φ, with Fourier coefficients depending on wind speed V and incidence angle θ.:

$$z(\theta, V, \phi) = B_0(\theta, V)^{0.625}[1 + B_1(\theta, V)\cos(\phi) + B_2(\theta, V)\cos(2\phi)]$$

Equation 2

CMOD5 is the GMF currently used for ERS. It is characterised by the B-parameters B_0, B_1 and B_2 (see Equation 2). A three-dimensional visualisation is possible where the x-, y- and z-axis represents the fore-, aft- and midbeam backscatter respectively. For a fixed incidence angle θ the GMF is a function of the two independent parameters V and Φ representing the wind speed and azimuth angle (i.e. wind direction with respect to antenna azimuth angle). The GMF forms a double cone surface as shown in Figure 3. The B_0, B_1 and B_2-parameter represent respectively the central “axis” of the cone, the ratio between the inner and outer cone surface radius, and the radius of the cone. The V-parameter scales along the central axis and the Φ parameter scales along the double circle. The black dots swarming around the cone represent measurements.

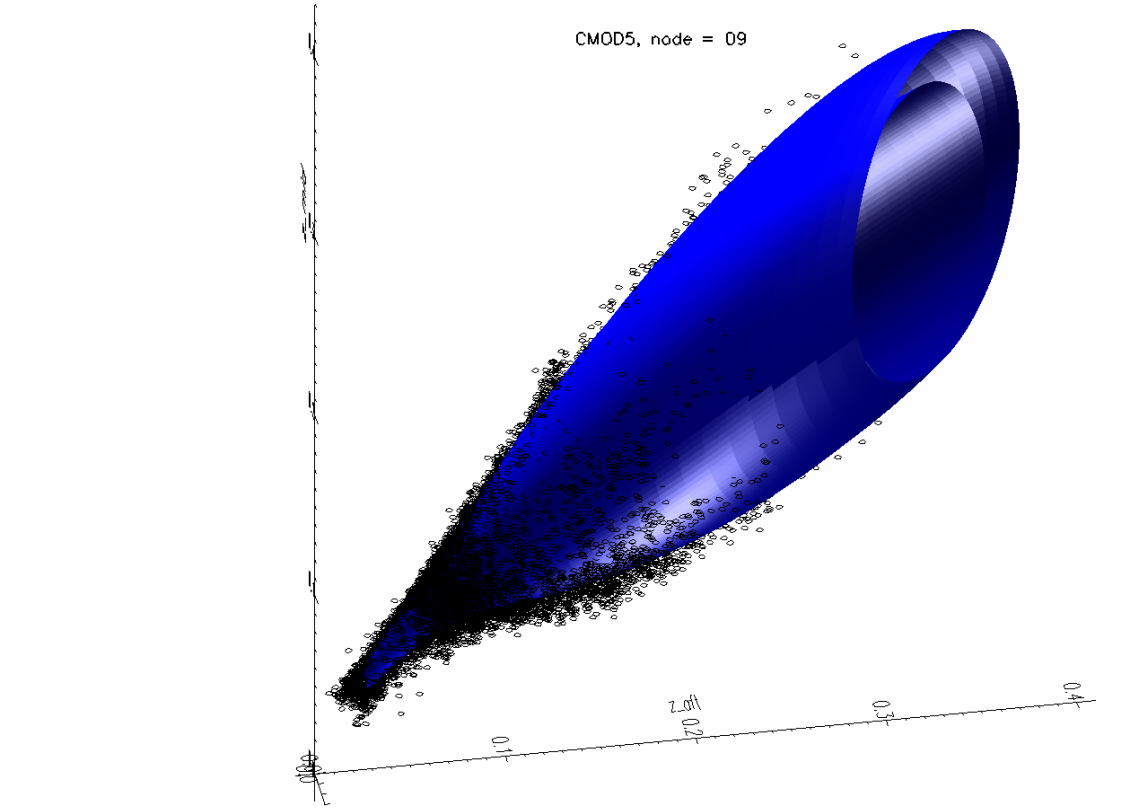

Figure 3 – CMOD5 wind cone with measured data points for node 9.

The Fourier expansion of a function f(x) is:

$$f(x) = \frac{1}{2} a_0 + \sum_{n=1}^{\infty} [a_n \cos(nx) + b_n \sin(nx)]$$

Equation 3

where the Fourier coefficients a_n and b_n can be written as

$$a_0 = \frac{1}{\pi} \int_{x=0}^{2\pi} f(x)\, dx$$

$$a_n = \frac{1}{\pi} \int_{x=0}^{2\pi} f(x) \cos(nx)\, dx, n=1,2,3,...$$

$$b_n = \frac{1}{\pi} \int_{x=0}^{2\pi} f(x) \sin(nx)\, dx, n=1,2,3,...$$

Equation 4

The Fourier coefficients a_n and b_n of the GMF are calculated by adequate integration on the ensemble measurements in z-space over the azimuth coordinate Φ. The Fourier coefficients and the parameters B_0, B_1 and B_2, will still depend on θ and V.

Equation 5

$$a_0(\theta,V)=\frac{1}{\pi}\int_{\phi=0}^{2\pi} z(\theta,V,\phi)\,d\phi$$

$$a_1(\theta,V)=\frac{1}{\pi}\int_{\phi=0}^{2\pi} z(\theta,V,\phi)\cos(\phi)d\phi$$

$$a_2(\theta,V)=\frac{1}{\pi}\int_{\phi=0}^{2\pi} z(\theta,V,\phi)\cos(2\phi)d\phi$$

$$a_n(\theta,V)=\frac{1}{\pi}\int_{\phi=0}^{2\pi} z(\theta,V,\phi)\cos(n\phi)d\phi=0, n=3,4,5,...$$

$$b_n(\theta,V)=\frac{1}{\pi}\int_{\phi=0}^{2\pi} z(\theta,V,\phi)\sin(n\phi)d\phi=0, n=1,2,3,...$$

The integrals are approximated by a weighted summation over measurements. In order to be able to do this the incidence angle, wind speed and azimuth angle are made discrete. The incidence angle of ERS and ASCAT has already discrete values by the definition of the level 1B WVC. For the wind speed V and azimuth angle Φ appropriate bins are defined which must be large enough to contain some measurements in each bin, and small enough to provide a good approximation of the integrals. A bin is indicated by index *i*, *j* and *k* for incidence angle, wind speed, and azimuth angle respectively. The calculation is also performed for each antenna separately to detect possible interbeam biases. For simplicity this is not indicated here. The Fourier coefficients of $z(\theta, V, \Phi)$ are approximated by the following weighted summation:

$$<a_0(\theta_i,V_j)>=2\sum_{q=1}^{N} z(\theta,V,\phi)\,w(V,\phi)$$

$$<a_1(\theta_i,V_j)>=2\sum_{q=1}^{N} z(\theta,V,\phi)\cos(\phi)w(V,\phi)$$

$$<a_2(\theta_i,V_j)>=2\sum_{q=1}^{N} z(\theta,V,\phi)\cos(2\phi)w(V,\phi)$$

Equation 6

The weight function $w(V, \Phi)=w(V_j, \Phi_k)$ may be taken inversely proportional to the probability $p(V_j, \Phi_k)$ that a certain measurement belongs to wind speed bin V_j and azimuth angle bin Φ_k. The weight function is calculated and normalised for each wind speed bin separately, such that it compensates for any dependency of the wind distribution on the azimuth angle Φ.

$$w(V,\phi) = \frac{p^{-1}(V_j,\phi_k)}{\sum_{q=1}^{N} p^{-1}(V_j,\phi_q)}$$
$$V_{lower,j} \le V < V_{upper,j}$$
$$\phi_{lower,k} \le \phi < \phi_{upper,k}$$

Equation 7

Here the subscripts *upper* and *lower* refer to the upper and lower limits of the bin respectively. As an example the wind distribution and weighting function from an actual calibration (see section 3.1.2) is shown in Figure 4. As can be seen in Figure 4a the wind direction distribution is different for each wind speed.

Figure 4b and Figure 4c show the normalised weighting function *w(V, Φ)* derived from Figure 4a, as a function of azimuth angle *Φ* and wind speed *V* respectively. The weighting function *w(V, Φ)* (see Equation 7) has a strong impact on the calibration results. In Figure 4b the average value of the normalised weighting factors is 0.33 because there are 30 azimuth angle bins. At low velocities there is a maximum at *Φ* =100º. For higher velocities this maximum diminishes and a second local maximum emerges at *Φ* =250º . Notice that maxima of the weight occur in Figure 4b at the location of minima of the wind distribution in Figure 4a. For high wind speeds the weight function is not shown here. Since these wind speeds do not occur frequently, their weighting function is irregular and peaked. Low sampling would lead to high errors in the wind speed distribution and weighting function. Therefore when the sampling gets too low, the weight factors for the whole wind speed bin is set to zero meaning that these measurements are not used.

Figure 4c shows the weight factors as a function of wind speed *V*. Note that the low and high wind speeds that are not frequently occurring get a relatively large weighting factor.

a)

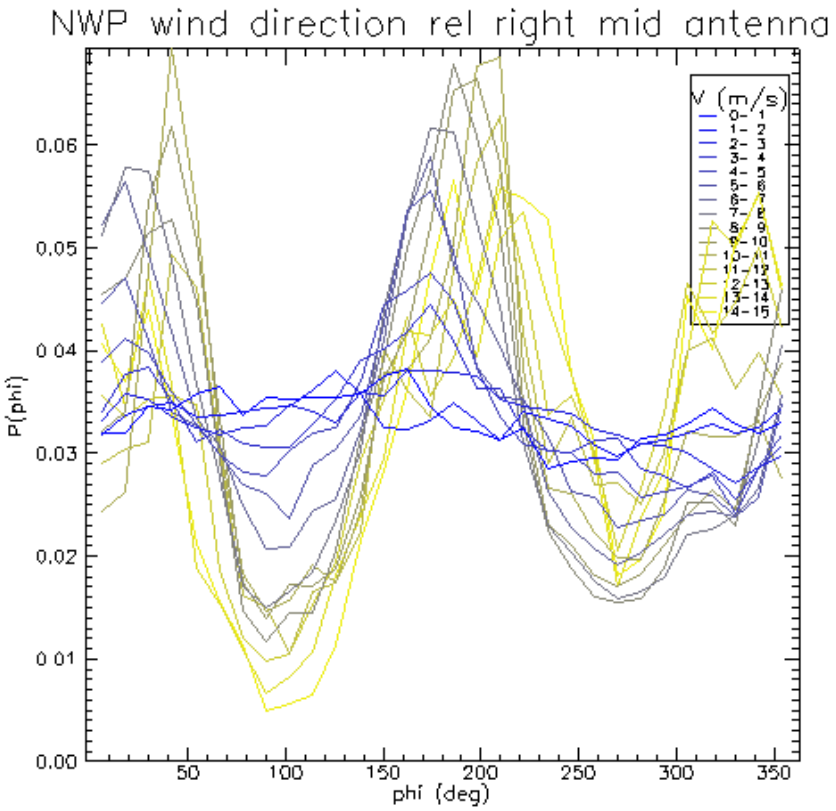
NWP wind direction rel right mid antenna
V (m/s)
0-1
1-2
2-3
3-4
4-5
5-6
6-7
7-8
8-9
9-10
10-11
11-12
12-13
13-14
14-15
P(phi)
0.00
0.01
0.02
0.03
0.04
0.05
0.06
50
100
150
200
250
300
350
phi (deg)

b)

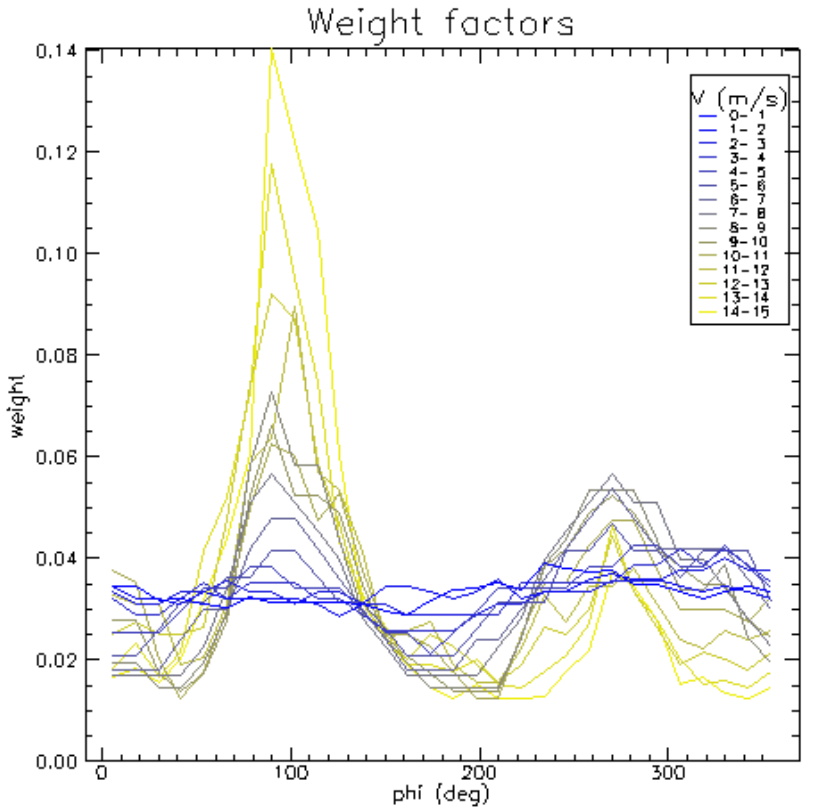
Weight factors
V (m/s)
0-1
1-2
2-3
3-4
4-5
5-6
6-7
7-8
8-9
9-10
10-11
11-12
12-13
13-14
14-15
weight
0.00
0.02
0.04
0.06
0.08
0.10
0.12
0.14
0
100
200
300
phi (deg)

c)

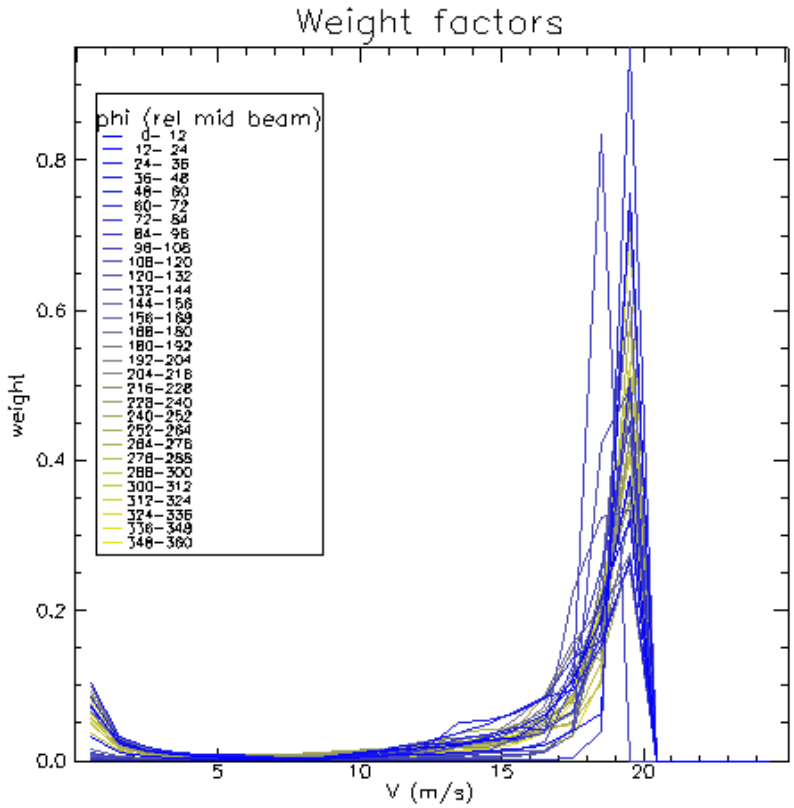

Figure 4 - Wind direction distribution and weighting factors from 1999-07
a) Wind direction distribution (azimuth angle relative to mid antenna)
b) Weighting factors derived form the wind distribution in a), as a function of azimuth angle.
c) Weighting factors derived form the wind distribution in a), aa a function of wind speed.

Once you have the Fourier coefficients the B-coefficients can be easily derived from them:

$$
\begin{aligned}
a_0 &= 2B_0^{\,0.625} \\
a_1 &= B_0^{\,0.625} B_1 \\
a_2 &= B_0^{\,0.625} B_2 \\
B_0 &= (\frac{1}{2} a_0)^{1.6} \\
B_1 &= a_1 / B_0^{0.625} = 2a_1 / a_0 \\
B_2 &= a_2 / B_0^{0.625} = 2a_2 / a_0
\end{aligned}
$$

Equation 8

The *a*- and *B*-coefficients are still a function of the wind speed V and incidence angle θ. The final step is to average over the wind speed bins:

$$\overline{B_n(\theta)} = \sum_{j=1}^{N_V} B_n(V_j,\theta)\, p(V_j)$$

Equation 9

Here $p(V_j)$ is the probability for wind speed bin V_j independent of parameter Φ. N_V is the total number of wind speed bins.

$$p(V_j) = N(V_j) / N_{tot}$$

Equation 10

Here $N(V_j)$ is the number of measurements in bin V_j and N_{tot} is the total number of measurements. Optionally a flat weighting may be chosen for the averaging over the wind speed bins:

$$p(V_i) = 1 / N_V$$

Equation 11

After averaging over the wind speed bins, the *a*- and *B*-coefficients are only dependent on the incidence angle.

3 Tools

3.1 Ocean calibration process

3.1.1 Code

An ocean calibration tool (oceancalib.x) has been developed that can process ERS as well as ASCAT data. Using the method described in section 2 the *B*-parameters are derived from the scatterometer measurements and from the collocated NWP winds. In effect a B_0-calibration consists of looking at the differences of averaged σ^0_M and σ^0_{NWP} over different cone section cuts (see Figure 3). Each wind speed bin V_i corresponds to a cone section cut. At the end of the process the *B*-parameters are plotted or the differences in *B*-parameters derived from scatterometer σ^0-s and NWP winds are plotted. In the end the plots are shown on a web page.

A schematic picture of the calibration process is shown in Figure 5.

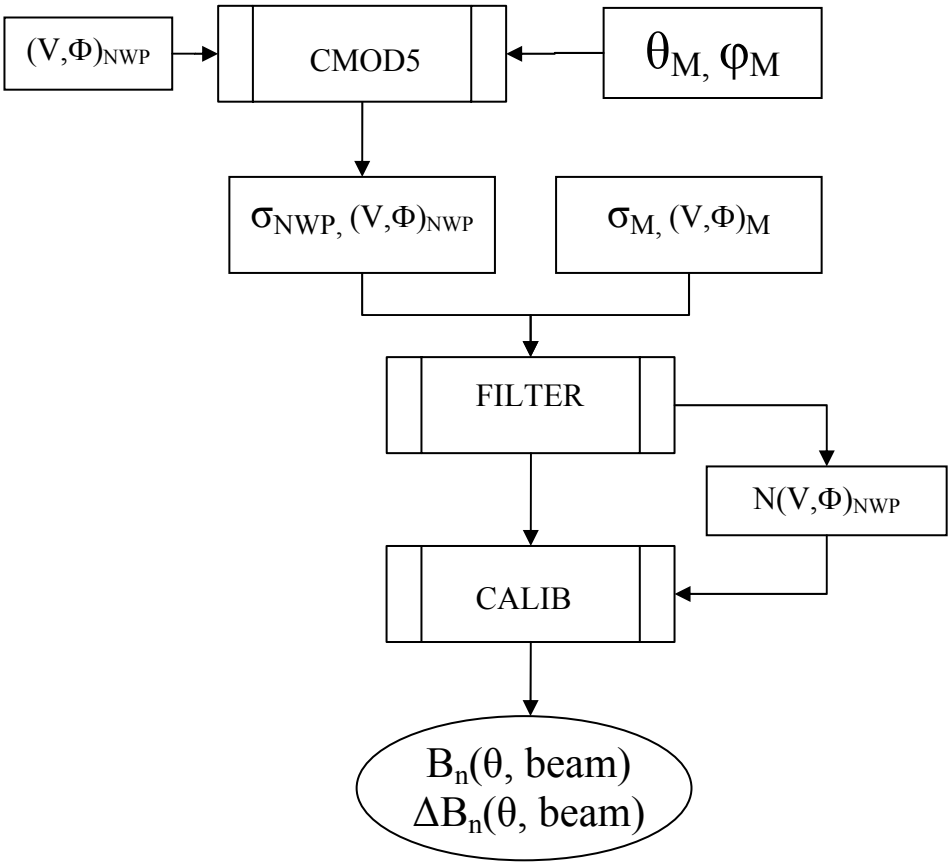

Figure 5 Schematic picture of the ocean calibration process

In the first run only the filter is applied in order to calculate the two-dimensional histogram $N(V_i, \Phi_j)_{NWP}$ with respect to the NWP wind speed and wind direction. It represents the number of occurrences of then NWP wind in bin (V_i, Φ_j). The result is written to file.

In the second run, the same filter settings are applied as in the first run. The NWP wind speed V_{NWP}, NWP wind direction Φ_{NWP} relative to the measured antenna azimuth angle φ_M, and measured incidence angle θ_M are used to calculate a simulated triplet of backscatter values σ^0_{NWP}.

The stored wind distribution is read and used for the calculation of the weighting function $w(V_i, \Phi_j)_{NWP}$. Together with the measured backscatter values σ^0_M and simulated backscatter values σ^0_{NWP} these are input for the actual calibration The output of this process are the Fourier coefficients a_n and the B_n-coefficients, as well as the differences between scatterometer and NWP derived B_n-coefficients. The calibration is done per incidence angle and per antenna in order to discover a possible interbeam bias.

Input - subroutine: readSigma()

A typical calibration takes from one day to one month of data. A meta inputfile specifies a list of BUFR files to be processed. The BUFR files are read in and processed sequentially and the intermediate cumulative results are stored. A BUFR file may contain one day of data.

Level 2 BUFR file(s) are needed which contain at least:

- σ^0_M , the measured σ^0
- θ_M, the measured incidence angle
- φ, the measured antenna azimuth angle with respect to North
- $(V, \Phi)_M$, the retrieved wind
- $(V, \Phi)_{NWP}$, the collocated NWP wind

In the calibration the azimuth angle $\Phi = \Phi_M - \varphi$ or $\Phi = \Phi_{NWP} - \varphi$ is used which is the angle between wind direction Φ and antenna azimuth angle φ. If only an order 0 calibration is done, i.e. only the B_0-coefficients are compared, then the retrieved wind azimuth angle Φ_M is not needed. Φ_M is only known after successful inversion and ambiguity removal and thus a valid σ^0-triplet is needed.

Filtering - subroutine filterBufrData()

For a successful calibration it is essential that only valid ocean points are considered. A conservative filter is used in here:

- lat/lon: based on the lat/lon coordinates points are filtered out that lie too close to the poles. Only points between latitude -55° and +65° are allowed. Also big lakes in North America and Siberia are filtered out, see[STOFFELEN 1998].
- Points with the land flag or ice flag set are filtered out.

Table 1 - *Filter options for BUFR data*

Filter name	Criterion for allowance
LatLon	latitude/longitude
Windspeed	wind speed in certain interval, e.g. V in [0, 4) m/s
Pole	Northpole/Southpole region
SatType	satellite type (ERS1, ERS2, METOP-A, METOP-B, METOP-C)
Ascending	Ascending orbit
Descending	Descending orbit
Distcone	$d_{cone} <= d_{max}$
Selection	a selected (retrieved) wind is present
Sigma	three valid σ^0-values are present
wvc_quality	Quality control (AWDP) is passed (testing on individual bits of the QC flag is possible)
s0_usability	usable σ^0-values are present (s0_usability = s0_good)
Kp	$K_p <= K_{p,max}$
IceProb	$P_{ice} >= P_{threshold}$
IceType	ice type (ice, sea, ice_or_sea, no_ice_no_sea)
QC	Quality control (ESDP) is passed (testing on individual bits of the QC flag is possible)
QCesa	Quality control (ESA) is passed (testing on individual bits of the QC flag is possible)
Mpc	missing packet counter, Mpc <= Mpc_{max}

Optionally other filtering criteria may be selected (see Table 1). The actually used filter options are written to the log file.

Binning - Histogram hist2dVPhi4mid represents the number of measurements $N(V, \Phi)_{NWP}$

For the weighted summation the backscatter values in z-space $z(V, \Phi)$ need to be binned with respect to wind speed V and azimuth angle Φ. Here Φ is the angle between the wind direction and the antenna azimuth. Normally the NWP wind relative to the mid antenna is used as a reference for the Φ-binning. The binning for the corresponding fore and aft antenna is the same in the case that only complete triplets are allowed by the filter. When incomplete triplets are

allowed, the wind distribution of the collocated NWP winds is different for each antenna and the binning is done for each antenna separately.

The size of the bins has to be chosen small enough for the weighted summation to be accurate but large enough to hold a significant number of measurements in each bin. This minimum required number of measurements in each bin N_{min} is set to 5. If it is not reached for a certain bin (V_i, Φ_j) then all the bins for that wind speed V_i are rejected. In this way it is assured that the summation over Φ-bins will give an accurate result. A bin size of 1 m/s for the wind speed V and a bin size of 12 degrees for the azimuth angle Φ are chosen as the default values.

V-bins : [0, 1), [1, 2),....., [24, 25).
Φ-bins : [0, 12), [12, 24),....., [348, 360)
N_{min} : 5

Note on binning BUFR parameters:
Parameters are stored with a certain precision in BUFR format, e.g. 10^{-1} for wind speed. After decoding, a 4 byte real variable containing the wind speed may have a value of $N*10^{-1}+10^{-6}$ or $N*10^{-1}-10^{-6}$. If the binning boundaries are a multiple of 10^{-1} these "machine number" errors of order 10^{-6} will have an effect on the binning, the wind distribution and thus on the calibration results. This could be overcome by shifting the bin boundaries by a small amount ε. Here ε must be chosen smaller than the precision with which the parameter is stored in BUFR, e.g. $\varepsilon = 10^{-3}$. When performing the binning ε is added to the wind speed.

Calculate the sets of σ^0-s - subroutine calc_sigma_beam()

The calibration structure (type Calib) arrays calMeas and calSim are calculated. Structure Calib is defined as:

```
type :: Calib
  real    :: z(n_sides, nBeam)
  integer :: iV, iPhi
  real    :: V                  ! windspeed
  real,   :: phi(nBeam)         ! winddirection relative to antenna
  real    :: weightVPhi         ! weight factor
end type Calib
```

This calibration structure contains z-values per antenna and per incidence angle, the binning indices, the wind speed and wind direction, and the weight factor. The z-values for calSim are calculated out of the NWP wind with the use of CMOD5, the V and phi values for calMeas are calculated out of the backscatter values with the use of inversion and ambiguity removal.

Calculate the Fourier coefficients - subroutine calc_weighted_sum_a()

With calibration structures calMeas or calSim as input, the weighted sum of the z and z^2 values are calculated (see Equation 6). Results are stored in a calibration set (type CalibSet):

```
type :: CalibSet
  character(len=5) :: id
                      ! identifier, e.g. 'meas', 'sim_', 'sim2'

  integer :: n_vbin  ! number of v-bins
  integer :: n_phibin! number of phi-bins
  integer :: n_nodes ! number of nodes
  integer :: n_sides ! number of sides (ERS: 1, ASCAT: 2)
  real    :: a(n_sides, nBeam, nParam, n_nodes, n_vbin)
  real    :: aSq(n_sides, nBeam, nParam, n_nodes, n_vbin) ! a^2
  real    :: B(n_sides, nBeam, nParam, n_nodes, n_vbin)
  real    :: BSq(n_sides, nBeam, nParam, n_nodes, n_vbin) ! B^2
  real    :: zNormTot(n_sides, nBeam, nParam, n_nodes, n_vbin)
```

```
            ! sum of weight factors over all used measurements

  real    :: aAve  (n_sides, nBeam, nParam, n_nodes)      ! a average
  real    :: aSqAve(n_sides, nBeam, nParam, n_nodes)      ! a^2 average
  real    :: BAve  (n_sides, nBeam, nParam, n_nodes)      ! B average
  real    :: BSqAve(n_sides, nBeam, nParam, n_nodes)      ! B^2 average
  real    :: BSd   (n_sides, nBeam, nParam, n_nodes)      ! B SD
  real    :: BAveMinusSd(n_sides, nBeam, nParam, n_nodes) ! BAve-BSd
  real    :: BAvePlusSd(n_sides, nBeam, nParam, n_nodes)  ! BAve+BSd
end type CalibSet
```

A calibration set contains the <a> and <B> coefficients, the <a^2> and <B^2> coefficients and a normalisation constant z_{norm} per incidence angle θ and antenna, which is the sum of all weight factors. These parameters are all resolved per antenna, incidence angle and wind speed bin. The calibration set also contains the a- and B-coefficients averaged over the wind speed bins, resolved per antenna and incidence angle.

Calculate the B-coefficients - subroutine calc_B()

When all input BUFR files are processed the <a>, <B>, <a^2> and <B^2> coefficients are normalised. Then with the Fourier a-coefficients as input the B-coefficients are calculated. (see Equation 8)

Average the coefficients over the wind speed - subroutine calc_Bave()

With the B-coefficients as input the averaging over the V-bins is performed (see Equation 9).

Ouput - subroutine writeCalibrationResults1()

The B-coefficients are written as a function of incidence angle and antenna to ASCII plotfiles. Note that the B_0-coefficient represents the average σ^0-value.

Output - subroutine writeCalibrationResults2(),

The B-coefficients from the NWP calibration set are subtracted from those from the measurement calibration set.

3.1.2 Output: ERS B_0-calibration example

The calibration software can handle a measurement set of σ^0_M triplets as input, together with collocated NWP wind vectors, from which σ^0_{NWP} triplets are generated using CMOD5 (see Figure 5). The reference run described here uses ERS-2 data from 1999-07. These data are collocated with NWP winds from ECMWF ERA40 and processed using AWDP (the ASCAT wind processor which can process ERS data as well) including a 2D-var ambiguity removal scheme. The data has been filtered beforehand excluding e.g. ice- and landpoints using conservative settings. In the calibration the points are weighted using the NWP wind distribution.

Figure 6a shows the average σ^0 as a function of incidence angle for the measured and the NWP set for the three ERS antennae. Also the average value plus or minus the standard deviation is shown in order to get an indication of the spread. The backscatter is a decreasing function of incidence angle θ. The range for the incidence angles is different for the fore- and aft antenna (24.8°-56.5°) and the mid antenna (18.0°-45.4°). The curves for the three antennae overlap well in the region where they have common incidence angles values (24.8°-45.4°). In a overlap is expected since the backscatter $z(\theta, V, \Phi)$ is calculated with CMOD5 where the incidence angle θ is an independent input parameter. No explicit dependency on antenna is present in CMOD5. In Figure 6b small deviations can be seen. Here the curves are weighted averages over the scatterometer measurements. Measurement triplets lie close to but not

exactly on the windcone because of instrument noise, geophysical noise and the error in the GMF. Moreover, any interbeam biases will show up in this figure.

Figure 7 shows the difference between measurement and NWP, i.e. Figure 6b-Figure 6a. The difference ranges from +0.2 dB to -0.4 dB. The plot shows large negative values for high incidence angles.

a)

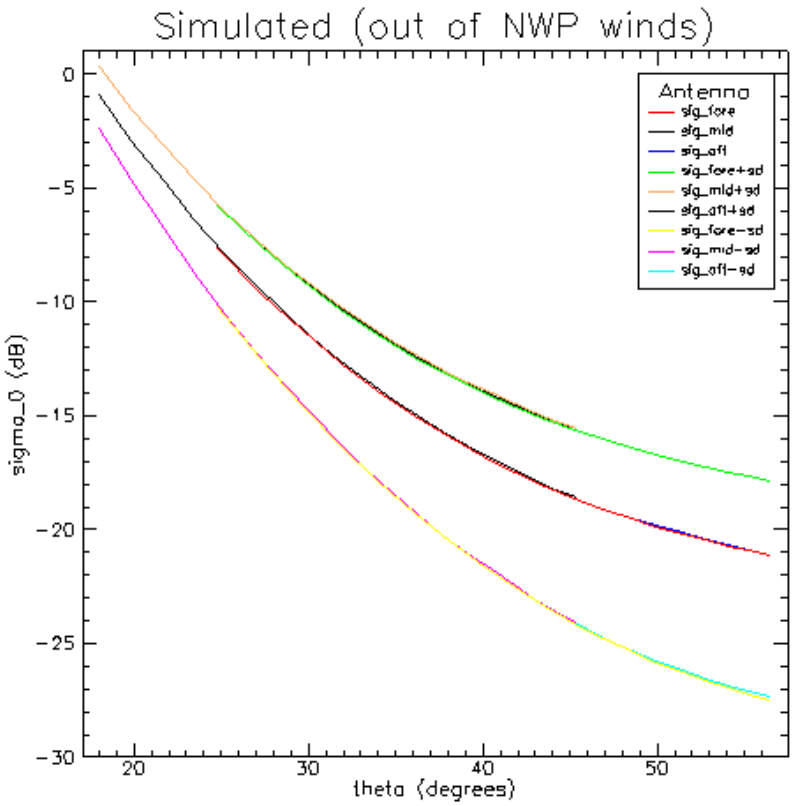

b)

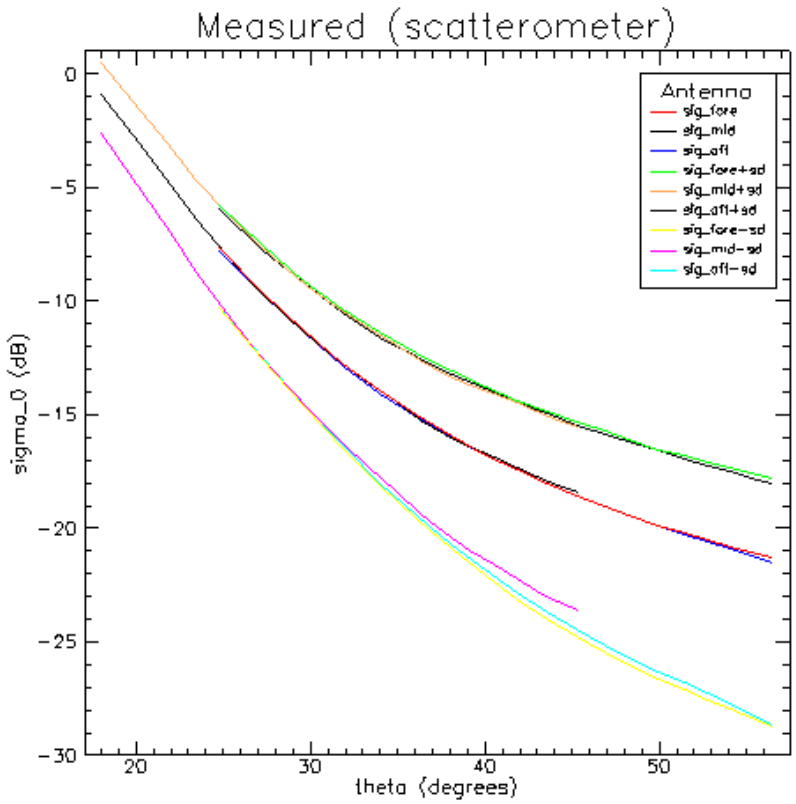

Figure 6 Average backscatter σ^0 as a function of incidence angle for the three antennae. Also the average value plus and minus one standard deviation (SD) is shown.
a) σ^0_{NWP} values derived from the NWP winds using CMOD5
b) σ^0_M values from the scatterometer

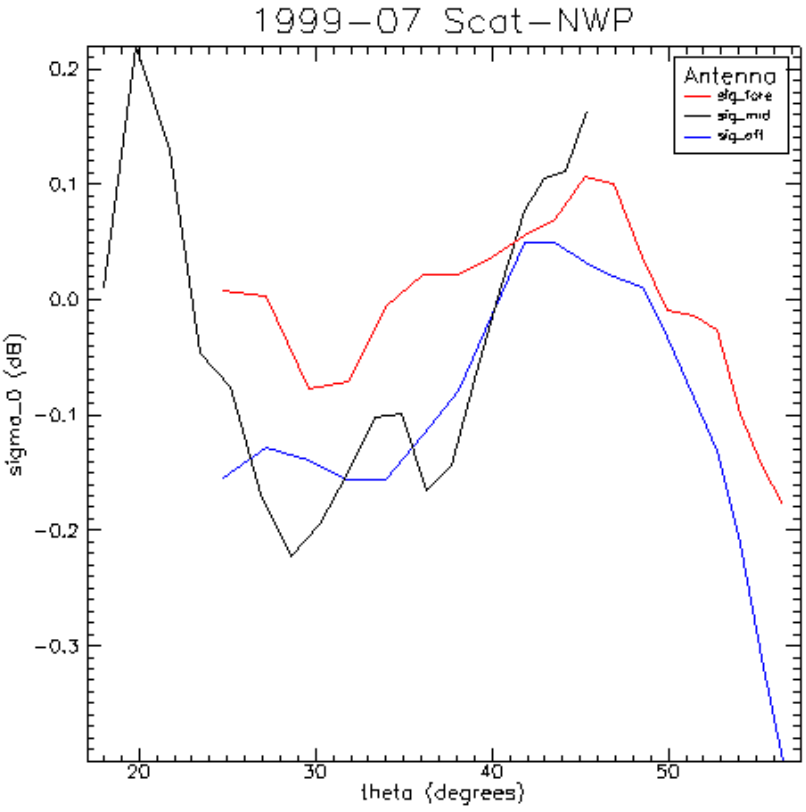

Figure 7 Difference in average backscatter σ^0 for the three antennae. Shown is the measured scatterometer σ^0 minus the σ^0 calculated out of the NWP winds (Figure 6b- Figure 6a).

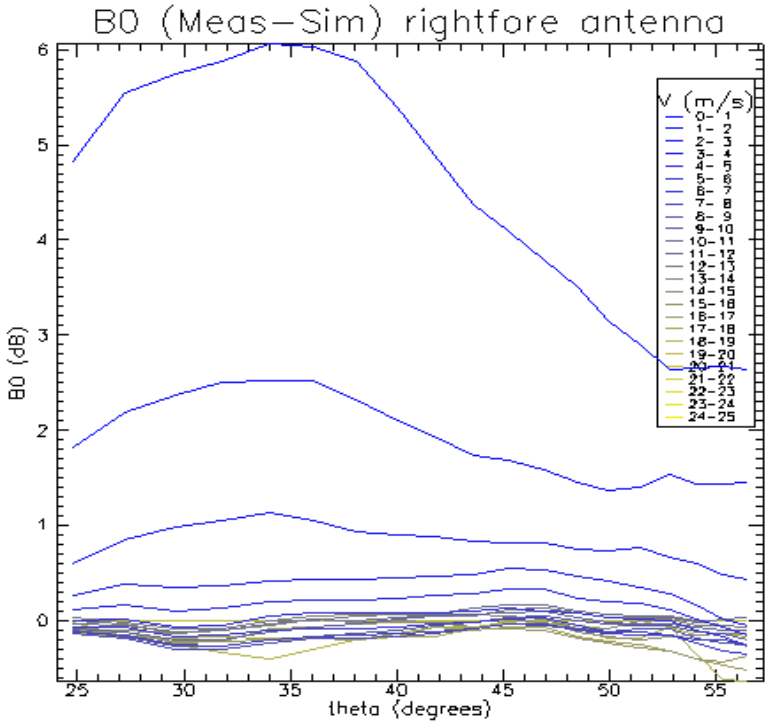

Figure 8 B_0 differences resolved per wind speed bin for the fore antenna

Figure 8 shows the B_0 differences resolved per wind speed class and incidence angle for the fore antenna. Large differences occur for the lower wind speed classes. The maximum difference is about 6 dB for the lowest wind speed bin. These differences can be explained by the error in the wind speed. The binning is based on the NWP wind speed only, for the lowest wind speed bin V_{NWP} in [0, 1) but the corresponding retrieved wind speeds V_M will have higher values on average. This effect of higher average wind speed is relatively the largest for the lowest wind speed bin (see [STOFFELEN 1998] section IV). Higher wind speed means more backscatter so the scatterometer B_0 is larger than the NWP B_0 value. If the retrieved wind speed would have been taken as a base for the binning, the NWP B_0 values would be the largest and the difference would have negative values (see section 4.3).

3.2 Simulation tool

A general purpose simulation tool (simulate.x) is developed for performing scatterometer software tests. The tool takes a BUFR file as input, perturbs the data in some way and writes another BUFR file as output, with the original data replaced with the perturbed data. Several options for perturbing the data are present. The most commonly used options are:

- A Gaussian error based on the geophysical and instrument noise may be added to the measured σ^0 -s, or to the σ^0-s derived from the NWP wind using CMOD5.
- Adding Gaussian errors to the NWP (u, v) wind components.
- Deriving σ^0 -values from the retrieved winds using CMOD5.
- Adding *B*-coefficient corrections to CMOD5. The corrections are read in from file.

The tool is based on the AWDP processor and perturbations can be performed two times per run independently on two places in the processing chain, before the inversion and after the ambiguity removal. A schematic picture of a possible simulation is drawn in Figure 9.

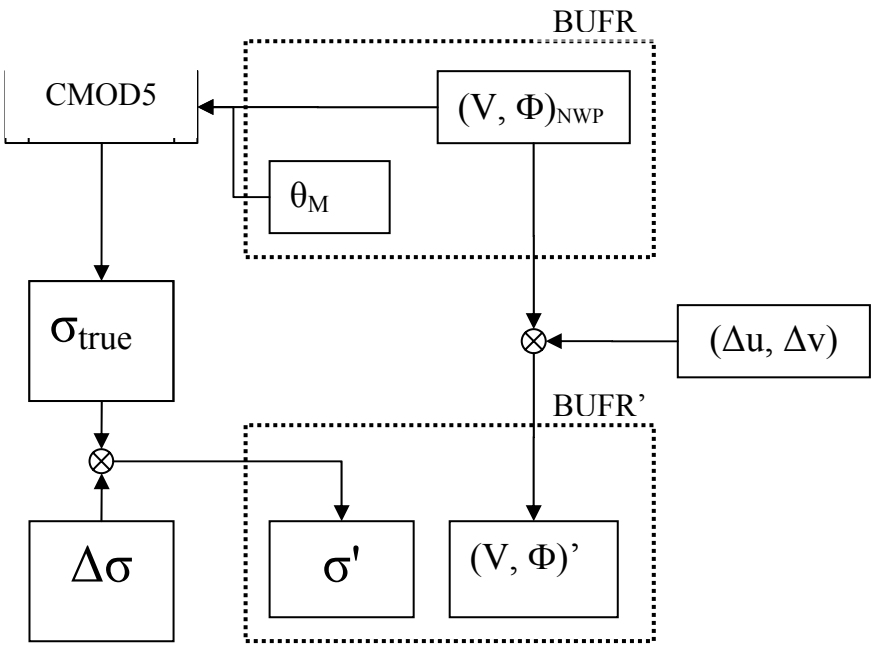

Figure 9 Schematic picture of the simulation tool

3.3 Analysis tool

An analysis tool has been developed (extract.x) that produces output in the form of histograms (probability distribution functions), graphical maps, statistical moments and visualisation files.

The tool takes one or more BUFR file as input (ERS or ASCAT) and filters the data using the same subroutine filterBufrData() as the calibration tool (see section 3.1).

Optionally the calculation uses a weight function that is derived from a wind distribution *N(V, Φ)* in the same manner as with the ocean calibration. The wind distribution *N(V, Φ)* has to be calculated and stored in a separate run.

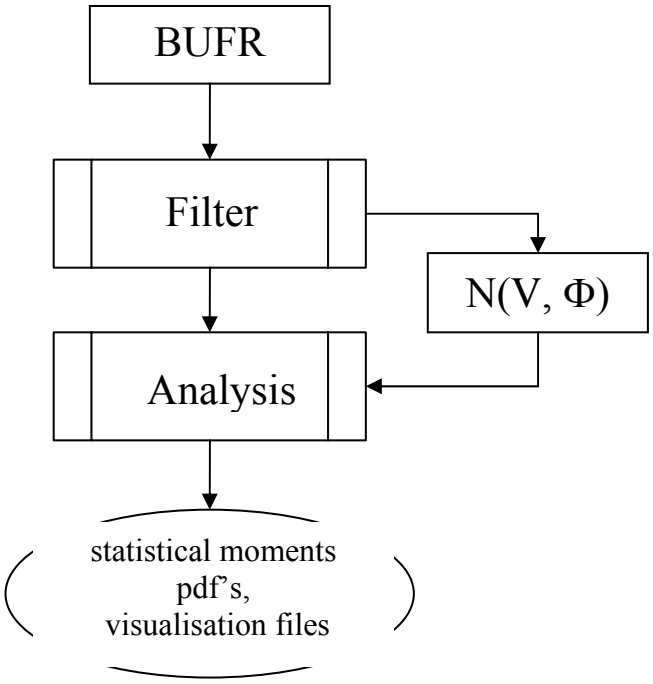

Figure 10 Schematic picture of the analysis tool

Output:
Histograms of many parameters

- backscatter σ^0
- node number
- incidence angle θ
- lat/lon
- wind speed V
- wind direction Φ
- (u, v) wind components
- distance to cone

Visualisation files are ASCII files (one file per node) which contain a limited set of parameters. These files are used as input for the visualisation tool that plots cone cross sections together with measured data points [VERSPEEK2006].

Statistical moments may be output with optionally using the weighting function.

Graphical files showing a parameter on the world map using a color scale. For the number of measurements *N(lat, lon)* this gives a fast indication of the coverage of the measurements.

4 Analysis

4.1 Characterising the input

In this section the distribution of the backscatter and the distribution of the wind is examined. These distributions are input for the calibration process and examining them will help in understanding the results.

Figure 11 shows the distribution of the backscatter signal for the mid beam (σ^0_{mid} in dB) resolved per node. The broadening of the curves is mainly caused by the wind. Also instrument noise and

geophysical noise contribute to the broadening. The curves are broader because both the σ^0 sensitivity to wind changes and the "radius" of the cone (or B_2-parameter) are larger than for low incidence angles. The distance between two peaks is decreasing with increasing θ which means that the backscatter wind sensitivity as a function of incidence angle is saturating. The calibration process looks at peak shifts in the order of a few tenths of a dB.

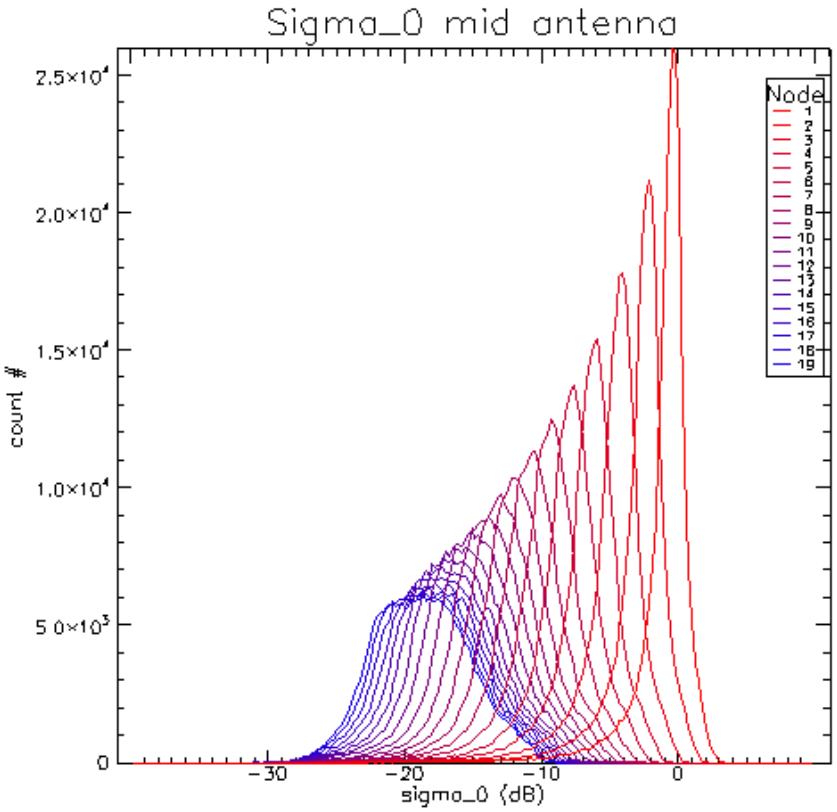

Figure 11 Distribution of sigma measurements from the ERS mid antenna in the month 1999-07 resolved per node.

CMOD5 will be used for incidence angles that were not used in the construction of CMOD5, although the lookup table used in CMOD5 covers the new range. In order to examine whether the extrapolation in CMOD5 towards the higher incidence angles is reasonable, a simulation of ASCAT data has been constructed. The NWP winds (collocated with ERS) are used to construct σ^0-values. Here the measured ERS incidence angle is replaced by an ASCAT incidence angle taken from a table. ASCAT has 21 nodes on each side in normal resolution mode. An experimental high resolution mode will have 41 nodes on each side with the size of the footprint halved. For ASCAT nodes 20 and 21, not present for ERS, a wind vector was generated using the average and standard deviation of the corresponding nodes 1 to 19. Thus a distribution of σ^0-values per node could be made for ASCAT. Compare Figure 12 with Figure 11.

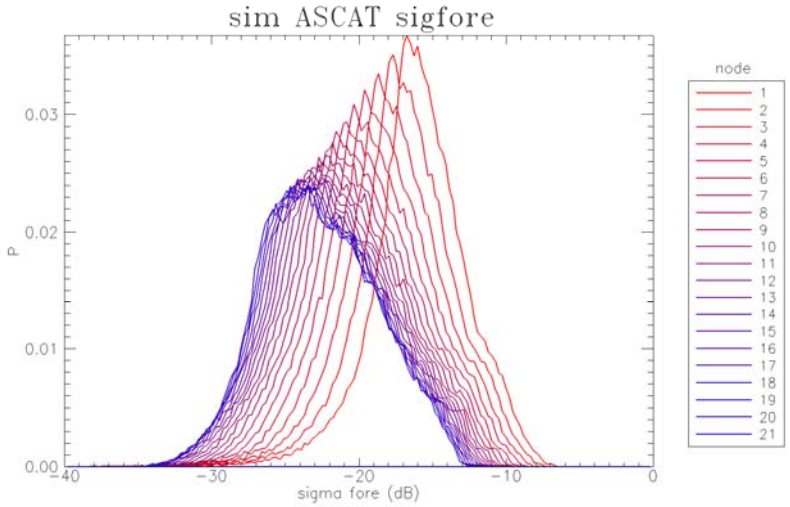

Figure 12 - Distribution of simulated σ^0 values for the ASCAT fore antenna resolved per node.

As can be seen the amount of shift of the distribution between two adjacent nodes is decreasing towards higher nodes. Also the shape does not change much anymore. It looks like the wind speed dependency of the backscatter is saturating.

It must be kept in mind that for the highest 7 nodes the simulation has been done with incidence angles for which CMOD5 is not yet verified. This has to be looked at in more detail when real ASCAT data are available.

It has to been seen whether the negative trend in backscatter difference (Figure 7) will be also present in the extended range of ASCAT incidence angles.

Figure 13a shows the distribution of the NWP wind components components (*u, v)*. The samples are collocated with the ERS measurements in the month 1999-07. As can be seen winds coming from the West are predominant. Figure 13b) shows the distribution of the the scatterometer winds. A second peak emerges for positive u values that is not present in the NWP wind distribution. This peak gives an indication of the fraction of wrongly selected wind solutions by the ambiguity removal.

a)

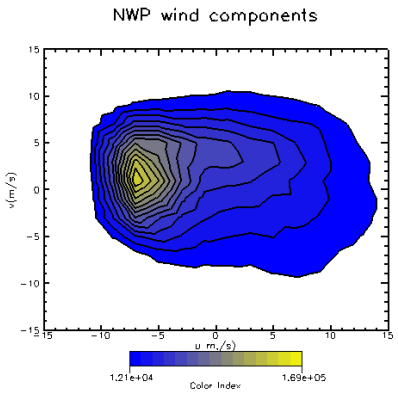

b)

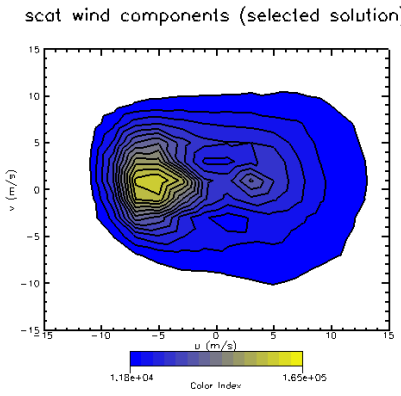

Figure 13- wind distribution (u, v) from the month 1999-07
a) NWP wind distribution (collocated winds)
b) Scatterometer wind distribution

Figure 14 shows the distribution of the measured and NWP wind components resolved per node. Ideally the distribution should be the same for each node. The measured *u*-distribution (West-East wind component) shows two maxima whereas the NWP *u*-distribution shows only one. The *v*-distribution (South-North wind component) of the retrieved winds shows a sharpening for low node numbers. This may be caused by a small dislocation of the GMF for low winds, which will favor a projection of the σ^0-triplet on the wind cone to a point with a low *v*-component (close to the plane $\sigma^0_{fore} = \sigma^0_{aft}$,)

a) b)

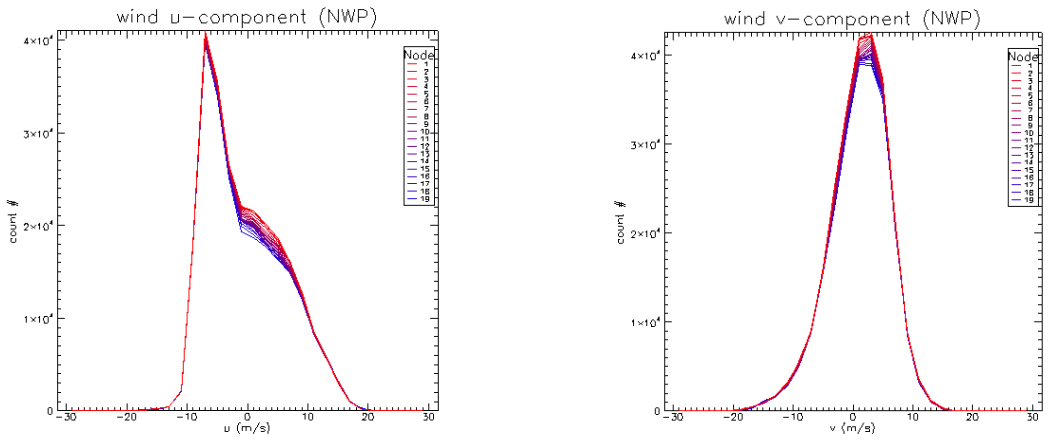

Figure 14 Distribution of the NWP wind components (1999-07)
a) *u* wind component b) *v* wind component

4.2 Characterising the weighting method

In Figure 15 and Figure 16 the difference between measured and NWP σ^0-value is shown for other methods of weighting in the Φ-direction. With the "weighted" method in Figure 7 the measurements are weighted inversely proportional to the number of measurements in the (V, Φ)-bin that that measurement belongs to (see Equation 7). With the "flat" Φ-method, the weighting function is flattened by throwing away surplus measurements. This is done for each wind speed bin V_j separately, in formula:

$$N(V_j, \phi_k) = \min_q N(V_j, \phi_q)$$

Equation 12

The flattening of the wind distribution can be obtained in two ways. Either a deterministic limit is used or a probability for rejection/acceptance for a measurement. In Figure 16a the acceptance/rejection of a measurement is done using a deterministic limit. When the limit is reached in a certain bin all new measurements in that bin will be rejected. In Figure 16b the acceptance/rejection is done using a random number generator. The advantage of a probabilistic acceptance/rejection is that possible spatial or temporal correlations are excluded beforehand. In practice there is hardly any difference between the two methods.

The “weighted” and “flat” methods give almost identical results (see Figure 7). These methods compensate beforehand for the non-homogeneity of the measurements in the Φ-direction. The “flat” method will have a somewhat higher error because not the full information content of the measurements is used. The “weighted” and “flat” methods are expected to give the same result.

a) b)

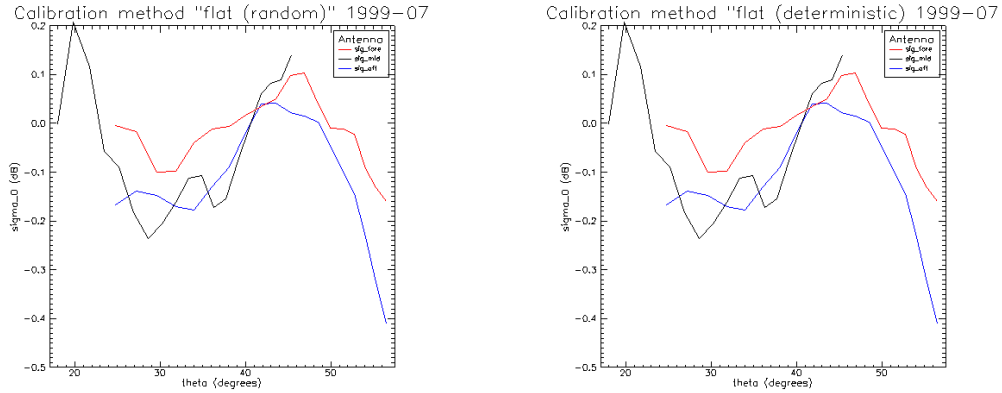

Figure 15 - Calibration results. Shown is the difference of the measured and the simulated backscatter resolved per incidence angle and antenna.
a) flat distribution forced, p(V, Φ) =constant, measurements are randomly dropped
b) flat distribution forced, p(V, Φ) =constant, measurements are accepted until limit is reached

In Figure 16 the “all” method is used, meaning all measurements are used with equal weight factor. The result of the “all” method differs from the others. The “all” method does not compensate for a possible Φ non-homogeneity, in some directions more measurements will be used than in other directions. When averaging all measurements along the double circle of the cone, the average value will in general not be in the center of the circle and will not represent the B_0-value. If you consider B_0-differences, not B_0-values, it is not clear beforehand whether there is an azimuth-dependency or not. If there would be no azimuth dependency, the result for the “all” method would be same as for the other methods.

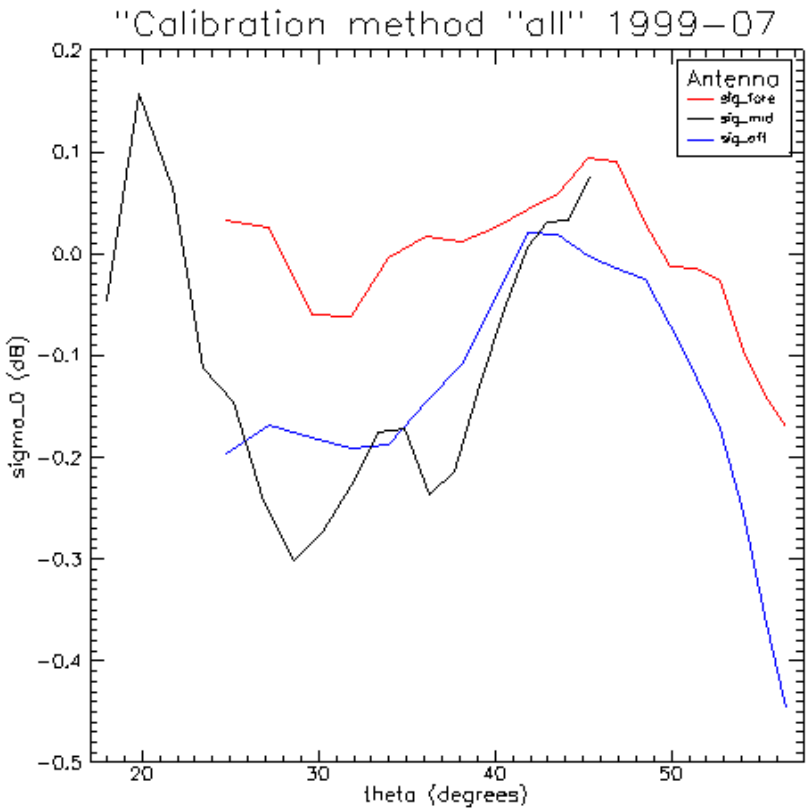

Figure 16 Calibration results. Shown is the difference of the measured and the simulated backscatter resolved per incidence angle and antenna. All measurements get equal weight.

4.3 Characterising binning

Figure 17 shows the calibration result in the case that the scatterometer wind distribution is used for the binning and for calculating the weighting factors. Compare this figure with Figure 7 where the NWP wind distribution is used. Figure 18 shows the B_0 differences resolved per wind speed bin (compare with Figure 8). Note that the average backscatter Figure 17 can be derived from Figure 18. It is the weighted average of B_0 over the V-bins. Although Figure 17 and Figure 7 do not differ that much, the difference between Figure 18 and Figure 8 is large. A difference in wind speed distribution between NWP winds and scatterometer winds will have great influence on the B_0-differences, especially for the low winds. The “reference” wind distribution (scatterometer) used for the binning will have a lower average wind speed for the lowest wind speed bins than the other wind distribution (NWP). This leads to the negative values in Figure 18. The effect is reversed for the highest wind speed bins where the wind speed average from the scatterometer is higher than from the NWP winds. This leads to the positive values in Figure 18.

.

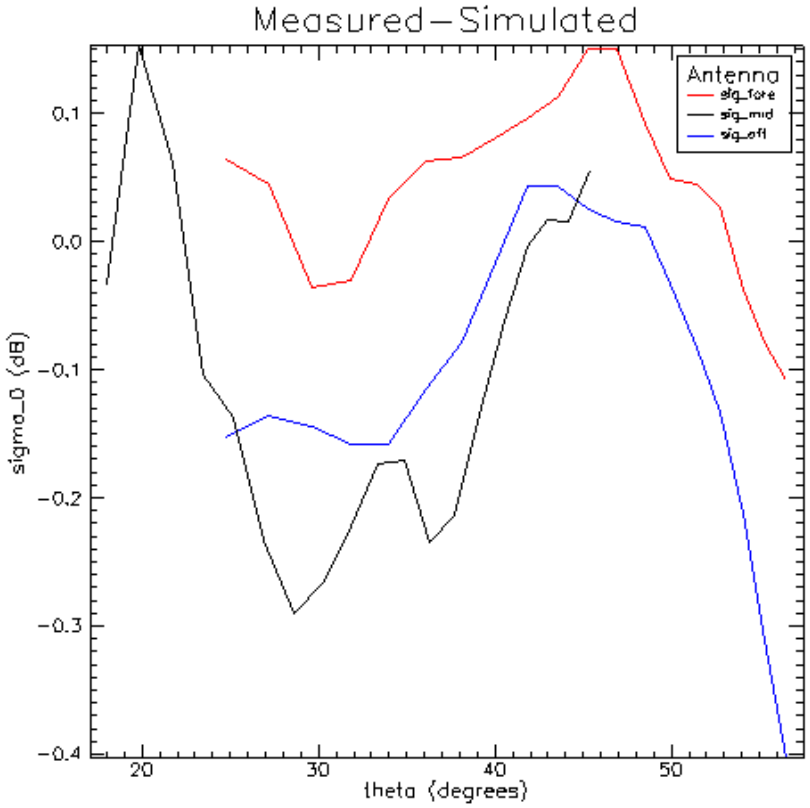

Figure 17 – Calibration results for the case where the retrieved winds are used for calculating the weighting factors. The difference between measured and NWP-derived backscatter is shown.

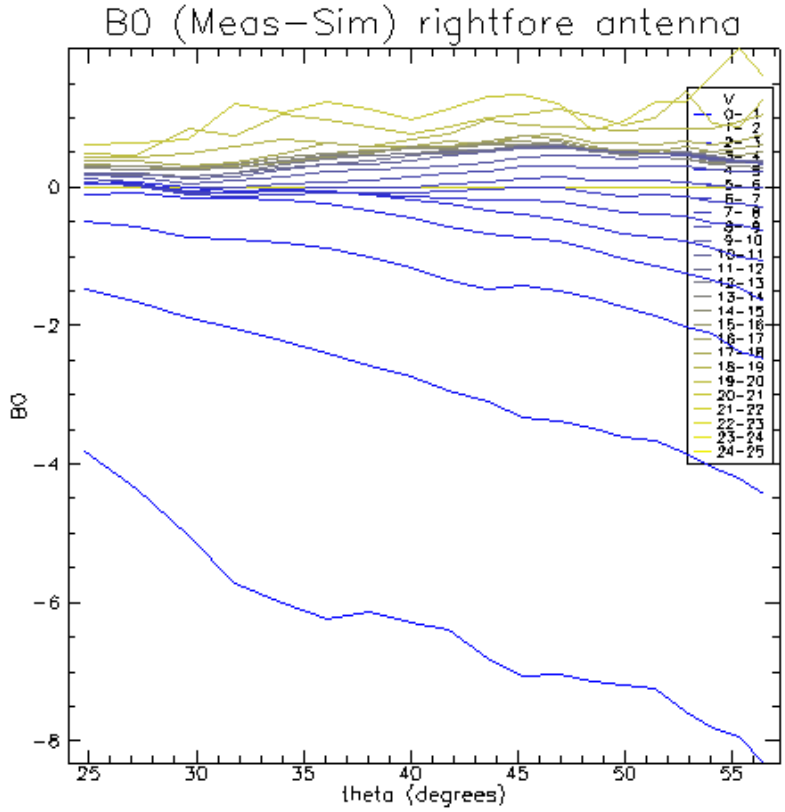

Figure 18 – B_0 differences per wind speed class and incidence angle for the fore antenna. The scatterometer wind distribution is used for the binning and the weighting function.

4.4 Uncertainty in the GMF

In order to get an idea of the influence of the GMF in the calibration, a comparison with an older version of the GMF is made. Figure 19 shows the calibration results with the previous version of the GMF CMOD4 (compare with Figure 7). The NWP has been multiplied with the CMOD4 calibration factor of 0.93 in order to compensate for the overestimation of the wind speed by the ECMWF NWP model with respect to the scatterometer winds (see [STOFFELEN 1998]). The CMOD4 GMF with multiplication factor gives comparable results in terms of absolute values to CMOD5, although the shape of the curves is quite different. A lot more can be said about the influence of the GMF on the calibration results. In fact the GMF is empirically determined by comparing the scatterometer data with NWP winds, so tuning the GMF is the key in getting good calibration results. When ASCAT data become available, the GMF has be assessed and when needed adapted for the extended incidence angle range.

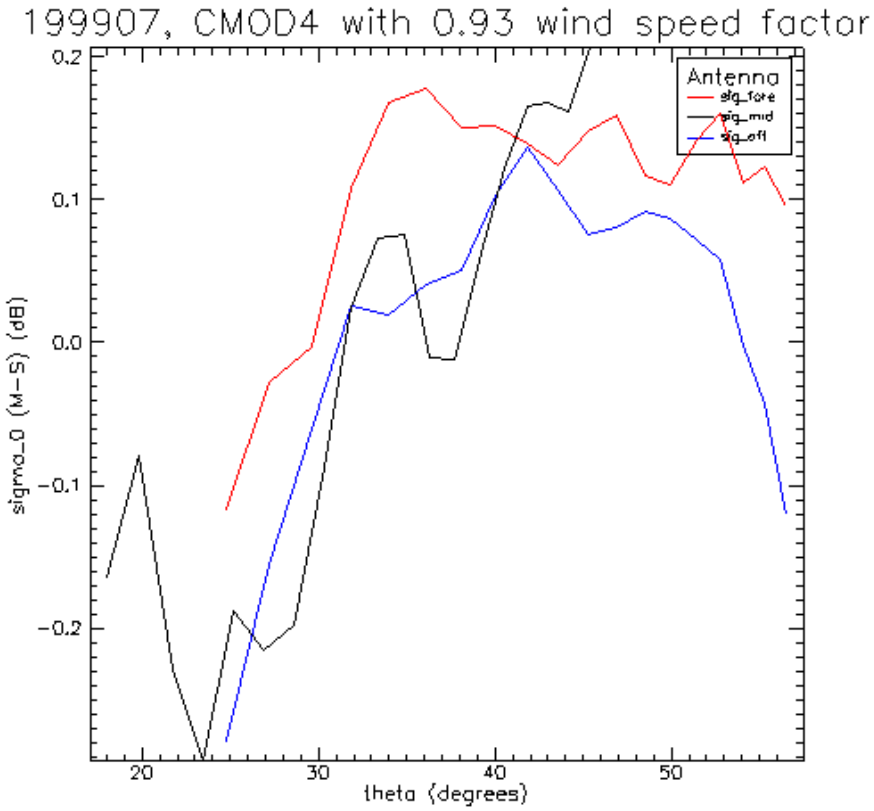

Figure 19 Ocean calibration for 1999-07 with CMOD4

4.5 Error analysis

In this section the results from several simulation runs will be discussed. The runs are derived from a reference run as starting point.

For ERS and ASCAT scatterometers an ocean calibration can be performed by comparing the measured σ^0-values with σ^0-values generated out of the collocated NWP wind field. Both measurement and NWP wind have errors. In order to examine the influence of these errors on the calibration result, simulations are run in which artificial but well known errors are added to one of the existing σ^0-triplet set.

For an adequate interpretation of the results from the calibration a simulated set of σ^0-values is used that is generated by adding a predefined error to one of the existing sets. The set to derive this simulated set from is either the set with scatterometer measurements or the set with NWP derived data. The error can be added in the σ^0 domain and/or in the wind vector domain. With the simulated set the influence of errors in GMF, NWP model and measurement can be studied in detail. The original set is declared as "truth" and the derived set with added noise is a simulated set. The simulated set is compared to the "truth" for verification or the ocean calibration procedure.

It turns out that errors in the wind domain have more impact on the calibration results than errors in the σ^0-values of the scatterometer measurements. This is due to strong non-linear effects in the GMF, for which the CMOD5 wind cone is used.

4.5.1 Combined errors

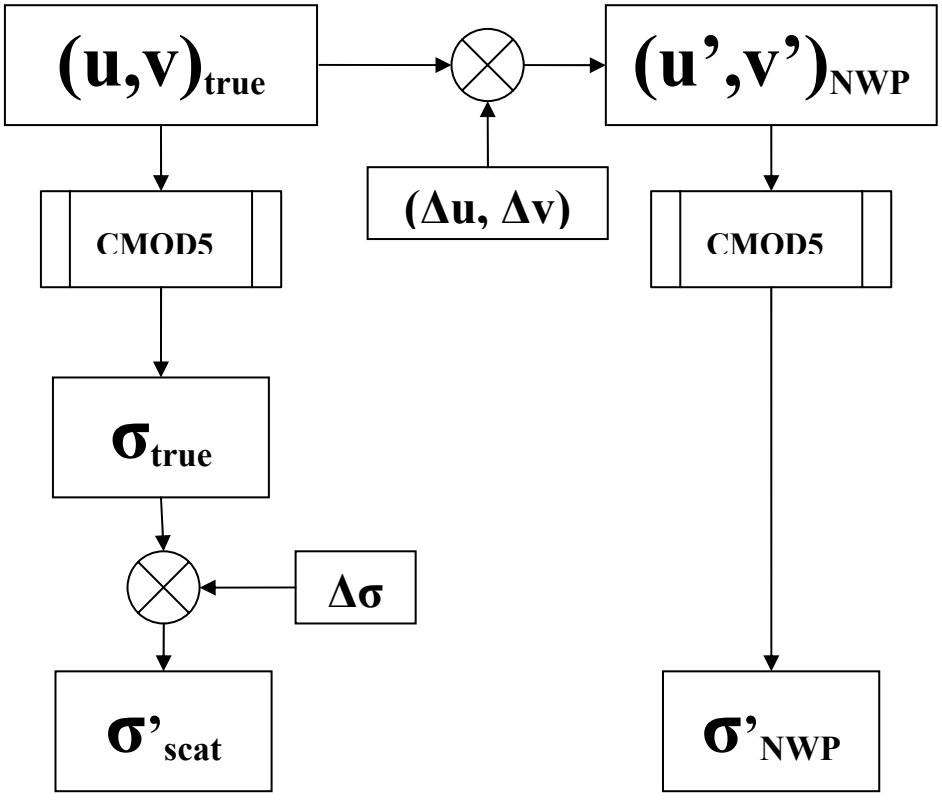

Figure 20 - Schematic picture of the combined errors

In this simulation both sets are derived from a "true" wind field $(u, v)_{true}$ that is defined by a gaussian distribution with a standard deviation of 6 m/s for both components. In one set (scat') errors are added to the σ^0-values, in the other set (NWP') errors are added to the (u, v) wind components. Figure 21 shows the results.

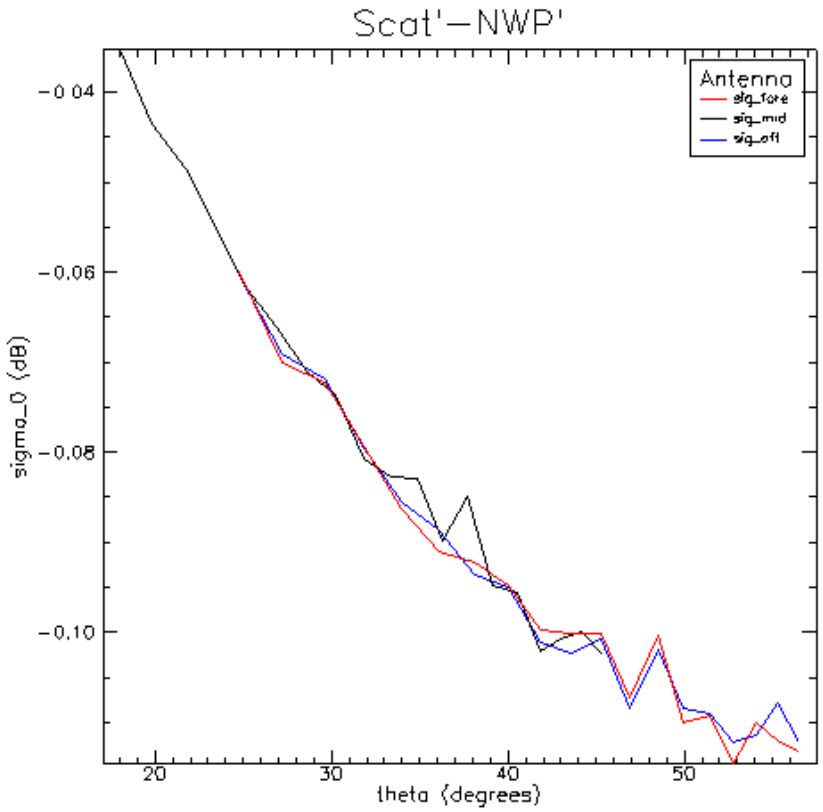

Figure 21 – Calibration results where a random error is added to the NWP derived σ0-triplets, and an error in the (u, v) wind components is added to the NWP wind components (single quote).

If you consider (u, v) to be the 'true' wind (which is unknown in reality) then σ' can be considered the NWP derived σ^0_{NWP}, and σ'' can be considered the measured σ^0_M. Normally the NWP wind distribution is used for calculating the weights, so in this case the NWP' is taken as a reference. The difference in results when taking the NWP (u, v) or the NWP' (u', v') distribution is very small though.

4.5.2 Adding an error to the NWP (u, v) wind components

In Figure 22 the wind distributions resolved per node are shown. In Figure 22a) one can see that the scatterometer wind speed is node dependent. This could be caused by a systematic error in the GMF with respect to the node number or incidence angle, but more likely it is caused by the fact that for low node numbers relatively more low winds and high winds are rejected by the quality control of the inversion and ambiguity removal [HERSCHBACH 2003]. This results in a more peaked, sharper distribution, also if you normalize the distributions. The NWP wind distributions are calculated independent of the measurements and cannot be dependent on node number. The slight node dependency in the NWP wind distribution (Figure 22b) is therefore caused by the collocation with scatterometer winds. The addition of the error to the NWP (u, v) wind components will have the effect that the original wind distribution (u, v) is convoluted with the distribution of the added errors (Δu, Δv). The original wind distribution is smoothed and slightly broadened
Figure 22c). Also the average wind speed is slightly increased. The low wind speed wing of the wind distribution will increase relatively strong.

a)

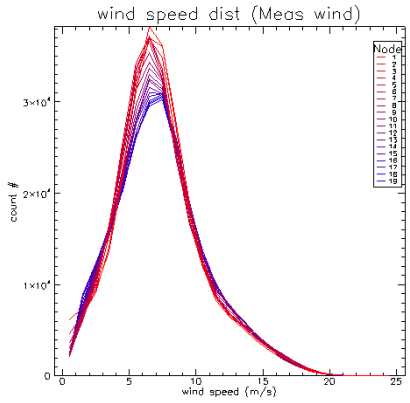

b)

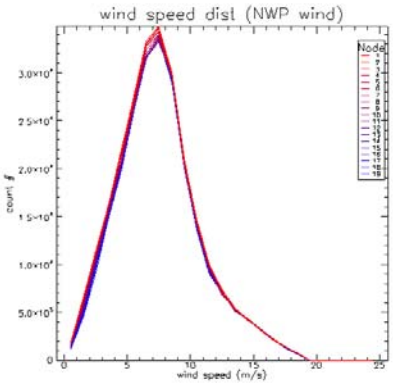

c)

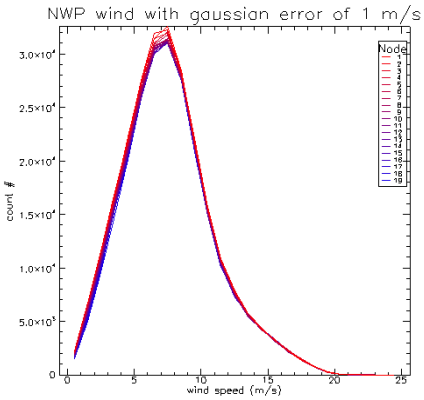

Figure 22 – Wind distributions per node from ERS data of 1999-07.
a) Scatterometer winds
b) Collocated NWP winds
c) Winds from a simulation where a Gaussian error of 1 m/s is added to the NWP (u, v) wind components.

Figure 23 shows the result from the 1999-07 calibration when a Gaussian error of 1 m/s is added to the (*u, v*) components of the NWP wind distribution. Figure 23c) shows the difference between NWP and NWP' (NWP with errors) derived σ^0-values. All values are negative because the addition of the error will increase the wind speed on average and thus the radar backscatter. If you assume the (*u, v*) wind components are Gaussian with a SD of *s* then the corresponding wind speed V will have a Rayleigh distribution with average wind speed V_{ave}

$$V_{ave} = s\sqrt{\frac{\pi}{2}}$$

Equation 13

which occurs at the maximum of the distribution. So the average wind speed is linearly dependent on *s*. When a standard deviation of *s* = 5 m/s in the (*u, v*) wind components is assumed to start with, adding an extra error of 1 m/s will increase V_{ave} by about 0.1 m/s. This increase causes an increase in the backscatter of about 10^{-1} dB for the high ERS nodes. For increasing incidence angle the backscatter is increasingly sensitive to the wind speed, which explains the shape of the curve. The random fluctuations on top of this curve are caused by the random fluctuations in the added errors. These fluctuations are in the order of 10^{-2} dB and are an indication of the effect of the error in the wind domain on the calibration.

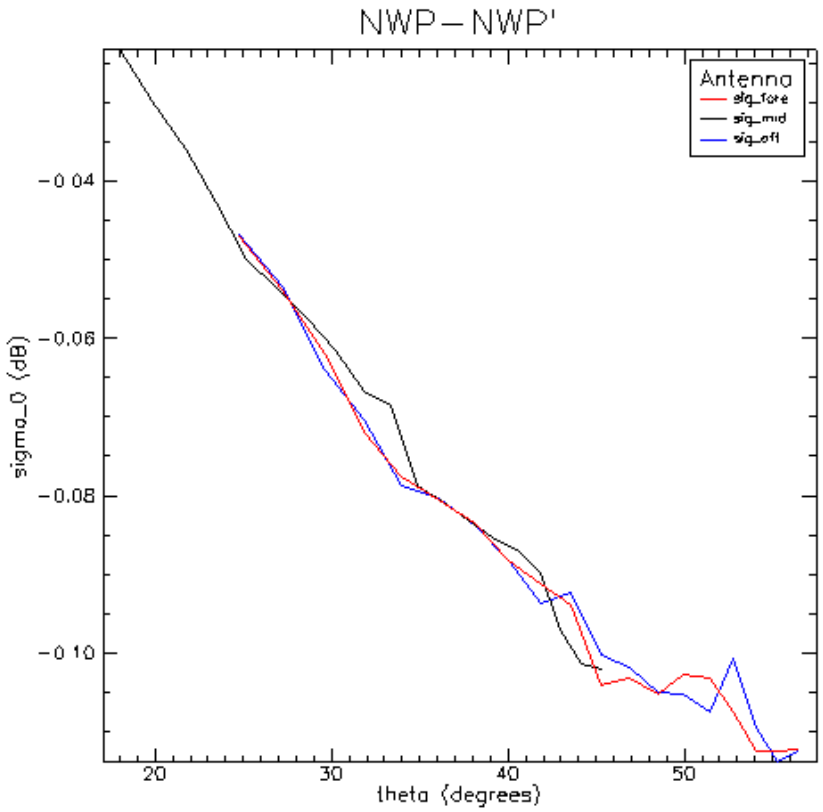

Figure 23 – Calibration results from ERS data of 1999-07. Shown is the difference in σ^0 (dB) as a function of incidence angle. NWP' refers to the NWP winds where a Gaussian error of 1 m/s is added to the (u, v) components .

Figure 24 shows the effect on the B_0 differences resolved per wind speed class and incidence angle.. This figure shows large values for the lower wind speed classes. This is caused by the fact that the increase in average wind speed is relatively the largest for the lowest wind speed bin (see also section 3.1.2). A wind speed error of 1 m/s gives rise to a maximum B_0 difference of -3 dB in the lowest bin. If you compare Figure 24 with Figure 8 the maximum difference of 6 dB can be accounted for by a wind speed component error of about 2 m/s (combined error for measurement and NWP wind), assuming the effect is linear.

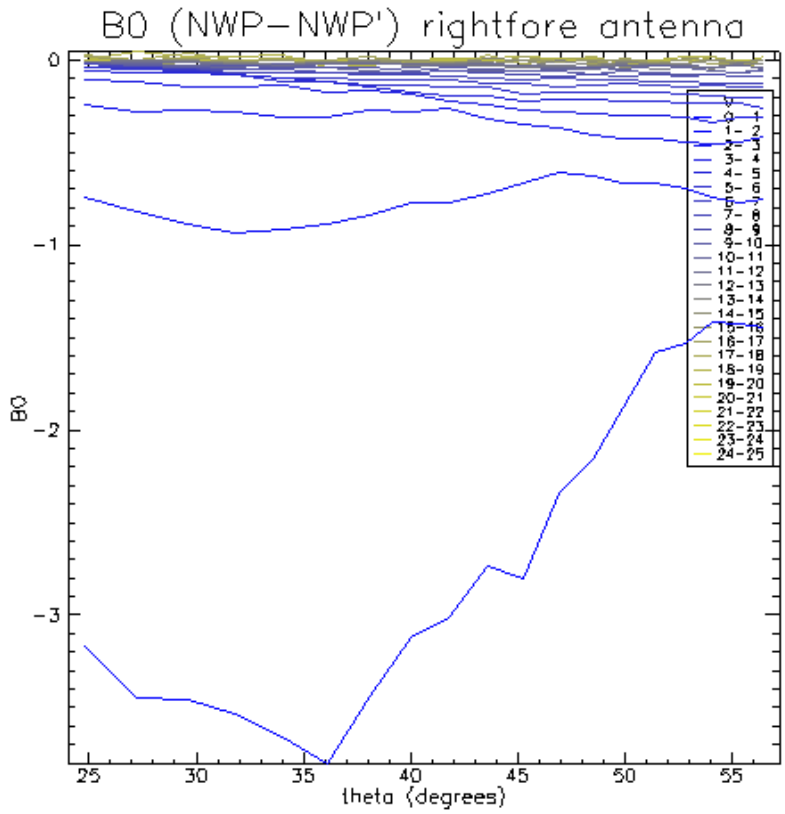

Figure 24 – B_0 differences per wind speed class and incidence angle.

4.5.3 Adding an error to the scatterometer σ^0 values

The error in the σ^0-triplet values from the scatterometer is split into two sources. The first source is the instrumental error Kp_{instr}. This error is caused by noise in the measurement and instruments itself. Its value is estimated from all σ^0-s contributing to an antenna σ^0 in a WVC, and written to the level 1B product. For ERS BUFR data before the 2003 gyro problem incident this value is not representative [PORTABELLA 2006], and instead the value is read from a table containing the mean instrument noise as a function of antenna and incidence angle.

The second source is the geophysical noise Kp_{geoph}. This error is caused by the wind variability within a WVC. The geophysical noise is read from a table as a function of wind speed and incidence angle. The combined noise level is typically 5 to 10 % [PORTABELLA 2006].

Figure 25 shows the results on the calibration. The effect of the errors in the σ^0-values on the calibration results is in the order of 10^{-3}. This is small compared to the effect of the error in the wind components which is in the order 10^{-2} (see section 4.5.2). This is due to the fact Kp errors are typically 5-10 %, while the NWP errors are typically 20 % or 3 to 4 times larger. Moreover, the Kp errors appear symmetrical, while the NWP errors are skew in wind speed and σ^0 for low wind speeds (symmetrical errors in the wind components leads to asymmetrical errors in the total wind speed).

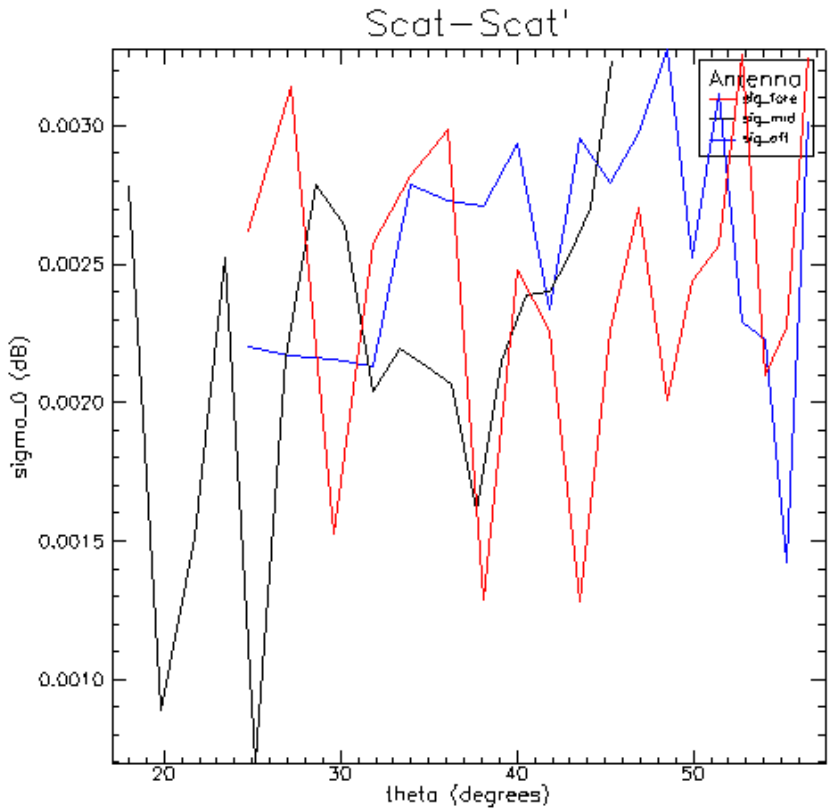

Figure 25 – Calibration results when a random Kp error (Scat') is added to the measured σ_0 (Scat).

4.6 Applying the calibration constants

The differences between the B_0-coefficients as calculated from the two sets of σ^0-values are called calibration coefficients. The calibration constants are a function of antenna and incidence angle or node. For ERS there are 3x19=57 calibration constants. Applying the constants is in effect the same as using a modified GMF.

Applying the calibration constants compensates for any systematic error in the calibration method, measurements, NWP winds and GMF. The calibration factors constitute a good interbeam calibration. In an absolute sense they are a measure of how well the agreement between model and measurements is. If the calibration factors are close to unity, it could mean that both are good, or that both are equally wrong.

The calibration corrections or modified GMF can be applied in advance to the inversion and ambiguity removal, when producing the level 2 wind product out of the level 1B product. This would result in a different distance to cone and possibly a different solution selected by the ambiguity removal procedure. Because the distance to cone has changed some points which were previously rejected by the quality control procedure may be accepted and vice versa.

In Figure 26a the calibration from December 1999 is shown . No new level 2 product was generated using AWDP but the original level 2 product was used generated with the ERS Scatterometer Data Processor (ESDP). Compared to the calibration of July 1999 (Figure 7) the shape of the curves resemble each other, even though the season for the two plots is different. This means that in principle the calibration results from one month could be used to improve the calibration results for forthcoming months.

In Figure 26b the calibration B_0-corrections from January 1999 were applied to December 1999. The used B_0-corrections were resolved per antenna and incidence angle. The correction

constants give a clear improvement even for this six month difference in time. The deviation is lower than 0.2 dB everywhere.

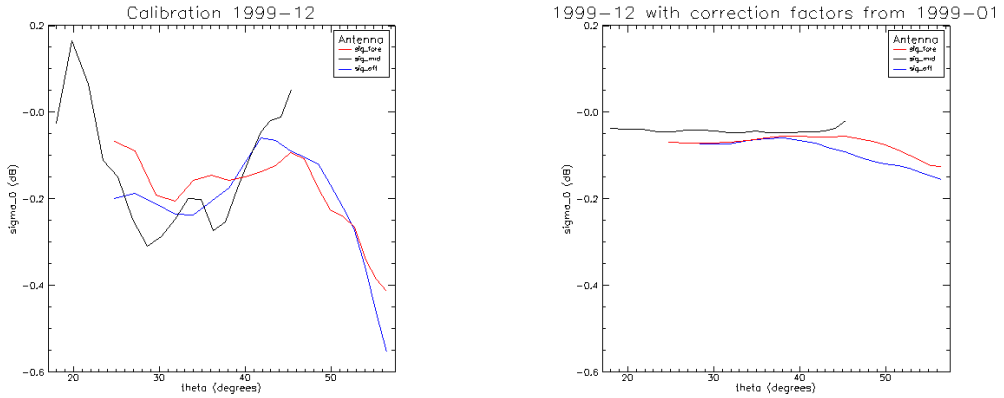

Figure 26 Ocean calibration results for
a) 1999-12
b) 1999-12 with corrections from 1999-01 applied.

5 Conclusions and outlook

An ocean calibration tool is developed for scatterometer data. The tool is primarily developed for the calibration of ASCAT but is able to handle ERS data as well. The method is based on fourier analysis of the data which is also used by [STOFFELEN 1998] and [HERSCHBACH 2003].

Several tests have been conducted with ERS data as input. The tests focus on B_0-calibibration. The weighting method used (flat or weighted according to wind distribution) has been tested. The results show deviations of a few tenth of a dB for both methods. Also the month-to-month ocean calibration results are robust and show little variation. This means that calibration correction factors from one month can be used to improve the result for forthcoming months. By doing so an absolute deviation smaller than 0.2 dB is obtained for all incidence angles and antennae.

Several simulations with added errors in wind domain and backscatter domain have been conducted. Realistic error models for the instrument and geophysical noise [PORTABELLA 2006] and NWP wind components [HERSCHBACH 2003] have been used. The simulations give an estimate of the influence of the errors on the calibration result. Errors in the backscatter domain give deviations in the order of 10^{-3} dB, errors in the NWP wind components give deviations in the order of 10^{-2} dB. If you consider the effect of absolute average wind speed differences deviations in the order of 10^{-1} dB are seen. It is found that an increase of 0.1 m/s in average wind speed results in a backscatter that is up to 0.1 dB higher.

When the calibration results are resolved per wind speed bin, large contributions to the end result can be seen from the lower wind speed bins. Deviations of 6 dB are present for the lowest wind speed bin: [0..1) m/s. The large contribution from low wind speed can be explain by the fact that for low wind speeds the error in the NWP wind components has a large effect on the error in absolute wind speed as well as wind direction. A simulation with a 1 m/s error added to the NWP wind components gives a deviation of 3 dB in the lowest wind speed bin.

Quality control in the inversion procedure can have an indirect effect on the ocean calibration. The selection or rejection of measurements is wind speed dependent and node dependent. The node dependency in quality control gives rise to a slight node dependency in the NWP wind speed distributions. Low wind speeds have a higher chance of being rejected. These effects result in a wind speed distribution that deviates from the true wind speed distribution. More work needs to be done to understand the differences between real and simulated data.

The tools for ocean calibration, data analysis and error analysis are ready for ASCAT. At the moment the tool is able to handle only complete measured triplets. The NWP wind distribution relative to the mid antenna is used for the calculation of weighting factors for all antennae. In order to be able to handle incomplete triplets, the wind distribution and weighting function must be calculated per individual antenna. The software will be adapted to do this.

Errors in the CMOD5 model function have not been examined in detail, but a comparison with CMOD4 has been made. Results for CMOD4 are in the same order as for CMOD5 when a multiplication factor is applied to the NWP wind speeds. A more detailed study has to be done when real ASCAT data becomes available. Because ASCAT uses higher incidence angles than ERS, the validity of CMOD5 for these new untested incidence angles has to be assessed.

Appendix A1 - Validation of the calibration software with a test function

Several tests have been performed to validate the calibration software and to get an indication of the accuracy of the method. A test function is applied to the Fourier analysis. The test function is sampled with a Φ-distribution that is flat, Gaussian, or according to the measurement distribution $w(V, \Phi)$. The results are given below.

Test function :

$$f(\varphi) = 25 + 10\cos(\varphi) + 5\cos(2\varphi)$$

19 runs with each approximately 100000 samples, corresponding to one month of ERS data $w(V, \Phi)$ distribution is used (with only 1 V-bin)

$$a_0 = 49.95719 \pm 0.065723$$
$$a_1 = 9.94520 \pm 0.20913$$
$$a_2 = 4.84895 \pm 0.16707$$

Appendix A2 – Comparision with original code

In order to test the software a comparison with the original ocean calibration software from [STOFFELEN 1998] has been performed. In order to get a clear comparison a number of alignment adaptations had to be made.

- The CMOD version, CMOD5 is built in the original code.
- The filtering has to be identical. E.g (no) ice filtering, filtering on ascending/descending orbit, filtering on the ESA quality flag, lat/lon filtering
- The wind calibration correction factor has been set to wind_cal = 1 (wind_cal = 0.93 in original code)
- The minimum number of measurements in any v bin needed for acceptation has been set to Nref_V_min = 5
- In “flat” mode, the original code uses a probabilistic criterion for accepting or reject a measurement. This has been changed to a deterministic criterion for making the comparison.
- The number of V-bins and Φ-bins have to be aligned, 1 v-bins was used, ranging from 0 to 20 m/s. For Φ 36 bins were taken, ranging from 0° to 360°.

With these mutual alignments the codes have been run with one day and one month of data, and the results turn out to be identical to within computational errors. Thus consistency with the original code has been confirmed.

Appendix B – Command line options

The software that is described in this report is developed in Fortran-90 and has been compiled with several compilers and run on Linux and Unix systems. A makefile is always available with the code. The programs have a lot of input parameters which may be optionally specified. When parameters are not specified by the user they will be given a default value. The modules and subroutines from genscat (generic scatterometer) and AWDP are reused when possible, e.g. for BUFR handling the genscat software is used.

The software resides in CVS on the bclap1 machine, in repository NWPSAF and module icemodel. The latest version can be retrieved with the command:

>vbcvs checkout –P icemodel
or
>cvs -d :ext:'logname'@bclap1:/data/cvs/nwpsaf checkout -P icemodel

Appendix B1 – oceancalib.x - command line options

This program is described in detail in section X.

`oceancalib.x [option] <optionValue>`

with <> indicating non-obligatory input, [] indicating obligatory input, and | indicating alternatives. The following command line options are available:

`[-i|--in] <metainfile>` Specify meta inputfile containing the list of BUFR files to be processed.

`[-if] <bufrinfile>` Specify a BUFR input file to be processed.

`[-o|--out] <outputfile>` Specify ASCII outputfile

`[-cmod] <4|5>` CMOD version to be used

`[-normmode] <all|flat|weighted>`
Normalising mode

`[-v_phi_infile] <vphiInfile>`
Input file containing (V, phi) distribution

`[-refSet] <0, 1, 2>`
Defines which wind distribution is used for the

	calibration weighting factors. =0: Scatterometer winds, =1: NWP winds, =2: Simulated set (SIM2) winds.
[-sim2option] <0..7>	
	Defines which simulation option to use for SIM2 =0: No simulation, =1: Error in (u,v) NWP wind components, =2: Error to scat sigma0 from FoM table, =3: Error to scat sigma0 from formula for geophysical noise, =4: Sigma0 value calculated from retrieved winds, =5: Sigmas calculated from NWP winds, added gaussian noise to sigmas, then invert, then calculate sigmas again out of inverted wind. =6: sigmas calculated from NWP winds, B-corrections (Scat-NWP) added from files. =7: sigmas calculated from NWP wind with added gaussian noise in (u, v). Then geophysical and instrument noise from table from FOM project added to the sigmas.
[-h|--helpall]	Shows command line options.
[-v|--version]	Shows version number
[-d|--debug] <debugLevel>	Debug level. =0 means no debug output.

Appendix B2 – simulate.x - command line options

The simulation software (see section X) is a stand-alone program that is an extension to the AWDP processor. All command line options from AWDP are reused and will not be described here. In addition to the ADWP command line options two extra command line options are available.

simulate.x [option] <optionValue>

[-simOption] <0..6>	Defines which simulation option to use before The inversion routine is called.
[-simoption2] <0..6>	Defines which simulation option to use after the ambiguity removal has been performed.

	=0: No simulation. =1: Gaussian error <delta> m/s added to the NWP (u,v) wind components. =2: Error to NWP sigma0 from FoM table. =3: Error to scat sigma0 from formula for geophysical noise. =5: Sigma0 value calculated from retrieved winds. =6: Gaussian noise added to the scatterometer sigmas. Standard deviation <delta> of noise is given as a fraction of the sigma0 value
[-delta] <delta>	Defines when needed a parameter that is used in the simulation option [-simOption], e.g. a standard deviation.
[-delta2] <delta2>	Defines when needed a parameter that is used in the simulation option [-simOption2], e.g. a standard deviation.

Acronyms and abbreviations

.

Name	Description
AMI	Active Microwave Instrument
ASCAT	Advanced scatterometer
AWDP	Ascat Wind Data Processor
BUFR	Binary Universal Form for Representation (of meteorological data)
CMOD	C-band geophysical model function used for ERS and ASCAT
ECMWF	European Centre for Medium-Range Weather Forecasts
ERA40	ECMWF 40 year reanalysis
ERS	European Remote sensing Satellite
ESA	Europeaan Space Agency
ESDP	ERS Scatterometer Data Processor
EUMETSAT	European Organization for the Exploitation of Meteorological Satellites
GMF	geophysical model function
KNMI	Koninklijk Nederlands Meteorologisch Instituut (Royal Netherlands Meteorological Institute)
METOP	Meteorological Operational satellite
MLE	maximum likelihood estimator
NWP	numerical weather prediction
QC	Quality Control (inversion and ambiguity removal)
SD	standard deviation
WVC	wind vector cell, also called node or cell

Table E.1 List of acronyms and abbreviations

References

[FIGA 2004] Figa, Julia, “ASCAT calibration and validation plan”, *EUMETSAT*, EPS programme, Darmstardt Germany, 2004

[HERSCHBACH 2003] Herschbach, Hans, “CMOD5 An improved geophysical model function for ERS C-band scatterometry, *Technical Memorandum 395, ECMWF*, Reading GB, 2003

[PORTABELLA 2006] M. Portabella, Study on an objective performance measure for spaceborne wind sensors (Figure of Merit) *KNMI progress report 2*, 2006

[JPL 2001] “QuikSCAT science data product user’s manual”, version 2.2, *Jet Propulsion Laboratory D-12985*, December 2001

[KLOE 2003] Optimisation of rotating, range-gated fanbeam scatterometer for wind retrieval, ESA/ESTEC I4383/00NL/DC, task 2a report, GMF and wind field definition, and wind retrieval, J.de Kloe, *KNMI* 2003

[STOFFELEN 1997] Stoffelen, Ad, “A simple method for calibration of a scatterometer over the ocean”, *KNMI*, PhD thesis, de Bilt, 1998

[STOFFELEN 1998] Stoffelen, Ad, “Scatterometry”, KNMI*, PhD thesis at the University of Utrecht*, ISBN 90-39301708-9, October 1998

[VERSPEEK 2006] Verspeek, Jeroen, “User manual Measurement space visualisation package”, *KNMI*, de Bilt, 2006